Determination of the Critical Slip Surface in Slope Stability Analysis

Muhammad Alizadeh Naderi

Submitted to the
Institute of Graduate Studies and Research
in partial fulfillment of the requirements for the Degree of

Master of Science
in
Civil Engineering

Eastern Mediterranean University
August 2013
Gazimağusa, North Cyprus

Approval of the Institute of Graduate Studies and Research

Prof. Dr. Elvan Yılmaz
Director

I certify that this thesis satisfies the requirements as a thesis for the degree of Master of Science in Civil Engineering.

Asst. Prof. Dr. Murude Çelikağ
Chair, Department of Civil Engineering

We certify that we have read this thesis and that in our opinion it is fully adequate in scope and quality as a thesis for the degree of Master of Science in Civil Engineering.

Assoc. Prof. Dr. Zalihe Sezai
Supervisor

Examining Committee

1 Assoc. Prof. Dr. Zalihe Sezai

2 Asst. Prof. Dr. Huriye Bilsel

3 Asst. Prof. Dr. Giray Özay

ABSTRACT

Analysis and design of the soil slopes has been an important field in geotechnical engineering for all the times. Various methods for analyzing two and three dimensional slopes have been created and developed based on different assumption and analysis methods. The factor of safety can be correctly obtained only if the critical failure surface of the slope is accurately identified. The critical failure surface for a given slope can be determined by comparing factor of safety of several trial slip surfaces. The slip surface that has the lowest factor of safety is considered to be the critical failure surface. The aim of slope stability analysis of any natural or manmade slope is to determine the failure surface that has the lowest factor of safety value. To find the minimum factor of safety, it is important to find the critical failure surface for the given slope. For that reason, different searching and optimization methods have been used in the past. However, they all carried almost the same limitation: They all had the difficulty in using them for hand calculations. In this study, effect of soil strength parameters on the failure surface and factor of safety of the slope were studied. Different slope stability analysis software programs were used and compared, and a formula was presented to calculate the length of failure arc by knowing the soil strength parameters. In this study, GEO5, SLOPE/W and FLAC/Slope software programs were used to analyze the slope stability problems and determine the critical failure surface. To investigate the validity and effectiveness of these programs, different values of shear strength parameters: cohesion (c), internal friction angle (ϕ), and soil unit weight (γ), were chosen and their effect on the factor of safety value were investigated. Additionally, an equation was introduced in order to locate the critical failure surface by using soils strength

and slope geometry parameters. Finally, the obtained results from different software programs were compared and discussed. The results of the study showed that the factor of safety of the slope changes with varying cohesion c, internal friction angle ϕ, and the unit weight γ of the soil. Moreover, the slip surface is affected by the dimensionless function λ which is related to the cohesion, internal friction angle and the unit weight. When λ is constant, the slip surface does not change along with the change of shear strength parameters. The obtained results showed that GEO5 is more conservative slope stability analysis software, compared to SLOPE/W. It gives 5% smaller factor of safety than SLOPE/W. On the other hand, FLAC/Slope usually gives out greater value for factor of safety compared to SLOPE/W and GEO5.

Keywords: Critical Failure Surface, Factor of Safety, Length of Failure Arc, Limit Equilibrium Method, Soil Slope Stability

ÖZ

Geoteknik Mühendisliğinde toprak kaymalarının analiz ve tasarımı her zaman için önemli bir alan olmuştur. İki ve üç boyutlu kaymaları analiz etmek için farklı varsayım ve analiz yöntemleri temel alınarak çeşitli yöntemler geliştirilmiştir. Emniyet faktörü doğru bir şekilde sadece yamaç kritik kayma yüzeyi doğru belirlenirse elde edilebilir. Belirli bir eğim için kritik kayma yüzeyi gelişigüzel seçilen birkaç kayma yüzeyinin güvenlik faktörünün karşılaştırması ile belirlenebilir. Emniyet faktörü en düşük kayma yüzeyi kritik kayma yüzeyi olarak kabul edilir. Herhangi bir doğal veya suni yamaç stabilite analizinin amacı yamaç emniyet faktörünün en düşük olan kayma yüzeyini belirlemek içindir. En düşük emniyet faktörünü bulmada, verilen eğimi için kritik kayma yüzeyini bulmak önemlidir. Bu nedenle, geçmişte farklı arama ve en iyi duruma getirme yöntemleri kullanılmıştır. Ancak, hemen hemen hepsi aynı zorluğa sahipdi: hepsi de el hesaplamarında kullanma güçlüğü taşımaktadır. Bu çalışmada, zemin mukavemet parametrelerinin kayma yüzeyi ve kayma emniyet faktörü üzerindeki etkisi çalışıldı. Farklı yamaç stabilite analiz bilgisayar yazılım programları kullanılmış ve karşılaştırılmıştır ve zemin mukavemet parametreleri bilenerek kayma ark uzunluğunu hesaplamak için bir formül sunulmuştur. Bu çalışmada, GEO5, SLOPE/W and FLAC/Slope yazılım programları yamaç stabilite problemleri analizi ve kritik hata yüzeyi belirlemek için kullanılmıştır. Geçerlilik ve bu programlarının etkinliğini araştırmak maksatı ile, farklı kayma gücü parametreleri: cohezyon (c), içsel sürtünme açısı (ϕ) ve toprak birim ağırlığı (γ), gibi parametreler seçilmiş ve bu parametrelerin emniyet faktörüne etkileri araştırılmıştır. Ayrıca, kritik kayma yüzeyininin yerini tayin edebilmek için zemin mukavemet parametreleri ve eğim geometri parametreleri kullanılarak bir

denklem tanıtılmıştır. Son olarak, farklı yazılım programlarından elde edilen sonuçlar karşılaştırılmış ve tartışılmıştır. Çalışmanın sonuçları göstermiştir ki değişen kohezyon c, içsel sürtünme açısı ϕ ve birim ağırlık γ değerleri ile yamaç emniyet faktörü değişmektedir. Ayrıca, kayma yüzeyi değeri, kohezyon, içsel sürtünme açısı ve zemin birim ağırlığını içeren boyutsuz λ fonksiyonu ile de etkilenmektedir. λ değerinin sabit olduğu durumlarda, kayma yüzeyi kesme gücü parametrenin değişimi ile değişim göstermez. Elde edilen sonuçlar GEO5 yazılım programının SLOPE/W yazılım programına göre daha muhafazakar yamaç stabilite analiz yazılım programı olduğunu göstermiştir. GEO5 yazılım programı SLOPE/W yazılım programına göre % 5 daha düşük bir güvenlik katsayısı vermektedir. Öte yandan, FLAC/Slope yazılım programı, GEO5 ve SLOPE/W yazılım programlarına göre genellikle daha yüksek güvenlik katsayısı değeri vermektedir.

Anahtar Kelimeler: Kritik Göçme Yüzeyi, Güvenlik Katsayısı, Göçme Ark Uzunluğu, Limit Denge Methodu, Zemin Yamaç Stabilitesi

To my beloved family
whose support,
this could not be done without

ACKNOWLEDGMENTS

I would like to express my utmost appreciation towards my dear supervisor, associate professor Dr. Zalihe Nalbantoğlu Sezai, with her countless guidance, helps, and comments during my study.

Also, I would like to show my deepest respects toward assistant professor Dr. Huriye Bilsel, whose guidance and comments during my “Special topics in Geotechnics” course were a prodigious guideline in my thesis.

TABLE OF CONTENTS

LIST OF TABLES

LIST OF FIGURES

LIST OF SYMBOLS/ABBREVIATIONS

- AutoCAD Automatic Computer Aided Design
- c Cohesion
- FEM Finite Elements Method
- FLAC Fast Lagrangian Analysis of Continua
- FS Factor of Safety
- h Height of Slope
- L Length of Failure Arc
- l_e Slope Surface Entry Distance
- LEM Limit Equilibrium Method
- UW Unit Weight
- α Angle of Slope (Figure 24)
- β Angle of Slope (Figure 24)
- γ Unit Weight
- λ Lambda (Equation 28)
- φ Internal Friction Angle

Chapter 1

INTRODUCTION

Wherever there is a difference in the elevation of the earth's surface, either due to man's actions or natural processes, there are forces which act to restore the earth to a levelled surface. The process in general is referred to as mass movement. A particular event of special interest to the geotechnical engineer is the landslide. The geotechnical engineer is often given the task of ensuring the safety of human lives and property from the destruction which landslides can cause.

Calculating the factor of safety, FS, of a slope, whether it is a natural slope or a man-made road embankment, is generally based on equilibrium of moments and/or forces.

The factor of safely in the category of slope stability studies is ordinarily outlined as the ratio of the final shear strength divided by the maximum armed shear stress at initiation of failure (Alkema & Hack, 2011). There are always deriving forces: weight of the rotating soil, surface loads and earthquake loads, and resisting forces: internal friction force and the cohesion of the soil at the failure surface and/or nailing resistance.

All of the methods of slope stability analysis discuss the forces, how to find, calculate and locate them to write the force and/or moment equilibrium and finally finding out the factor of safety by dividing resisting forces by deriving forces. To do

so, the engineers should guess the failure surface by themselves then apply one of the methods to find out the FS. Then, by hiring trial and error method, change the failure surface and recalculate the FS, and repeat this procedure until the minimum FS is found.

Since the very first studies carried out in order to determine the stability of the slopes, finding the critical failure surface has been an important issue. Lots of studies have been done on this subject, and there are number of searching technics available to use such as random methods (Boutrup & Lovell, 1980), grid counter methods (Bromhead, 1992), Siegel's method for non-homogenous slopes with a weak layer (Siegel, 1975), a technique established by Carter (Carter, 1971) for non-circular slips using Fibonacci sequence, Revilla and Castillo's method for non-regular failure surfaces (Revilla & Castillo, 1977), Nguyen's (Nguyen, 1985) and Celestina and Duncan's optimization techniques (Celestino & Duncan, 1981), Li and White's one-dimensional optimization method (Li & White, 1987), Baker's nodal points method (Raphael Baker, 1980), and more recent works by using genetic algorithms (Goh, 1999), simple genetic algorithm (Zolfaghari, Heath, & McCombie, 2005), Leapfrog algorithm (Bolton, Heymann, & Groenwold, 2003), annealing algorithm (Cheng, 2003) and etc.

But even today, after all these studies, most of the engineers prefer to use their experience to locate the slip surface. This is mostly because of hard methods, such as genetic algorithm, or time-consuming methods, such as trial and error.

1.1 Aims of the study

The specific aims of this thesis are as follows:

1- Perform a literature review to study the theatrical background of the most widely used slope stability analysis methods as well as critical failure surface searching techniques.
2- Evaluate the effects of soil strength and slope geometry parameters on the factor of safety and critical failure surface using different slope stability analysis software programs.
3- Perform comparison between the results of these different slope stability analysis software programs.
4- Correlate and formulate the relation between soil strength and slope geometry parameters and critical failure surface and achieve a numerical formula to locate the critical slip surface.

1.2 Research Outline

This study comprises 5 chapters. The first chapter describes the aim of this research and the background information on the slope stability and its analysis methods. The second chapter covers a review on the literatures on the slope failure surface searching methods. In the third chapter, methods and software programs as well as materials which have been used in this thesis will be demonstrated. The fourth chapter will present modelling results and full discussion on them. In the fifth chapter, conclusions of this thesis will be provided and afterwards, references and resources of this research will be presented.

1.3 Background

1.3.1 Slope

Slope is referred to an exposed ground surface that stands at an angle with the horizontal (Das, 2010). The slope can either be man-made like road embankments and dams or natural. A schematic view of a soil slope is presented in Figure 1.

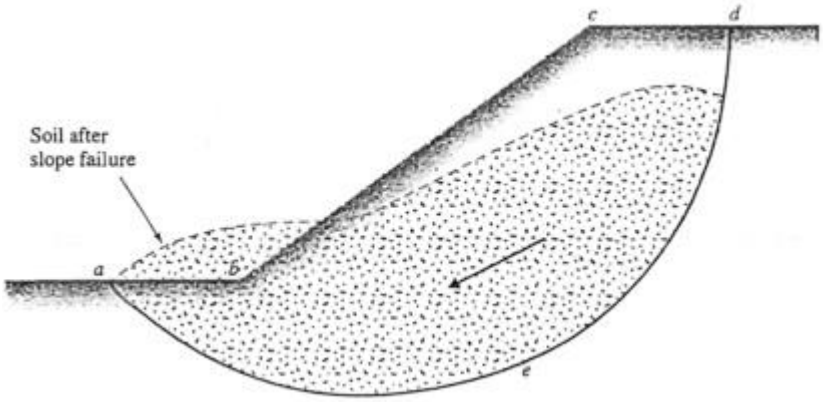

Figure 1. Schematic Diagram of Failure Slope (Das, 2010)

Slopes often get unstable under the deriving force of gravity and/or the overhead surcharges. Instability of slopes also have different types of triggers such as earthquake (Hack, Alkema, Kruse, Leenders, & Luzi, 2007) and (Jibson, 2011) and infiltration (Cho & Lee, 2001) or even evaporation of the soil humidity (Griffiths & Lu, 2005).

1.3.2 Factor of Safety

The factor of safety is usually introduced as the result value of dividing the resisting over deriving forces. There are numerous methods of formulating the factor of safety, usually each of the analysis methods has its own formula for FS, but the most common formulation for FS assumes the FS to be constant along and can be divided into two types; Force equilibrium and Moment equilibrium. (Cheng & Lau, 2008)

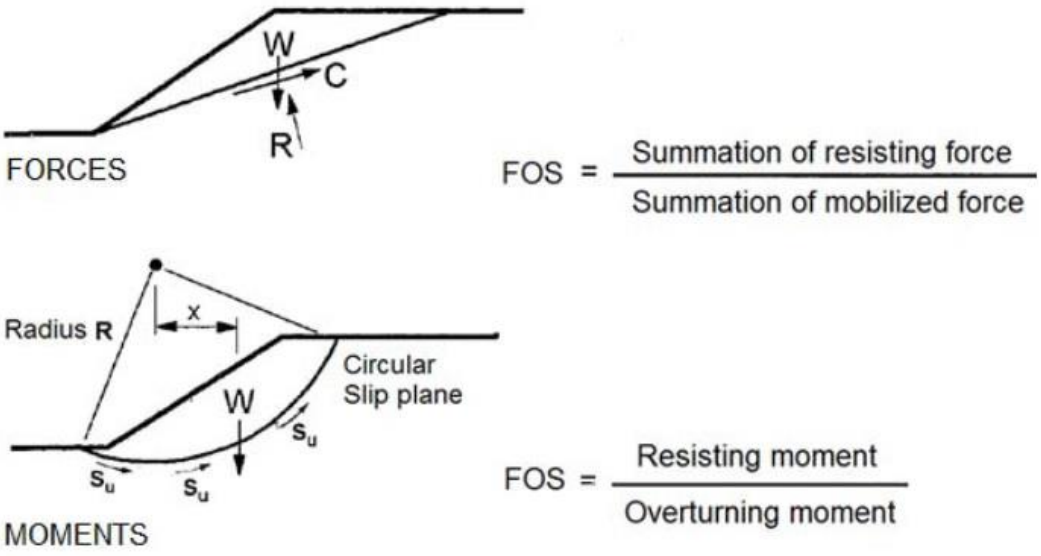

Figure 2. Different Methods of Defining FS (Abramson, 2002)

where: W is weight of soil

c is cohesion

S_u is total stress strength

R is resisting force

x is weight moment arm

Chapter 2

LITERATURE REVIEW

2.1 Introduction

In this chapter, studies on slope stability analysis methods, and slip surface seeking approaches and relations between location of failure surface and soil strength parameters will be presented.

2.2 Slope Stability Analysis Methods

There are several different methods available to use in order to analyze the stability of a slope. At present time, no single one of the analysis methods is preferred over others thus reliability of any solution is completely left to the engineer in charge (Albataineh, 2006).

These methods are divided into two major groups based on their main procedure;

A Limit Equilibrium Methods and

B Finite Element Methods.

Each of these methods are subdivided into two groups regarding their numbers of dimensions; two-dimensional and three-dimensional methods.

2.2.A Limit Equilibrium Methods

2.2.A.1 Two-Dimensional Methods

This group can also be subdivided into three different groups;

2.2.A.1.1 Circular Methods,

2.2.A.1.2 Non-Circular Method and

2.2.A.1.3 Methods of Slices.

2.2.A.1.1 Circular Methods

2.2.A.1.1.1 Swedish Circle

The Swedish Circle method (otherwise known as $\varphi = 0$) is the simplest technique of analyze the short-term stability of slopes disrespect to its homogeneous or inhomogeneous state.

This method analyzes the stability of the slopes by two simple assumptions; a rigid cylindrical block of soil will fail by rotating around its center with an assumption of internal friction angle being zero. Thus, the only resistance force or moment will be the cohesion parameter and the deriving force simply will be the weight of the cylindrical failure soil.

In this technique, the factor of safety has been specified as division of resisting moment by deriving moment (Abramson, 2002). Figure 3 shows the resisting and deriving forces acting on the soil block.

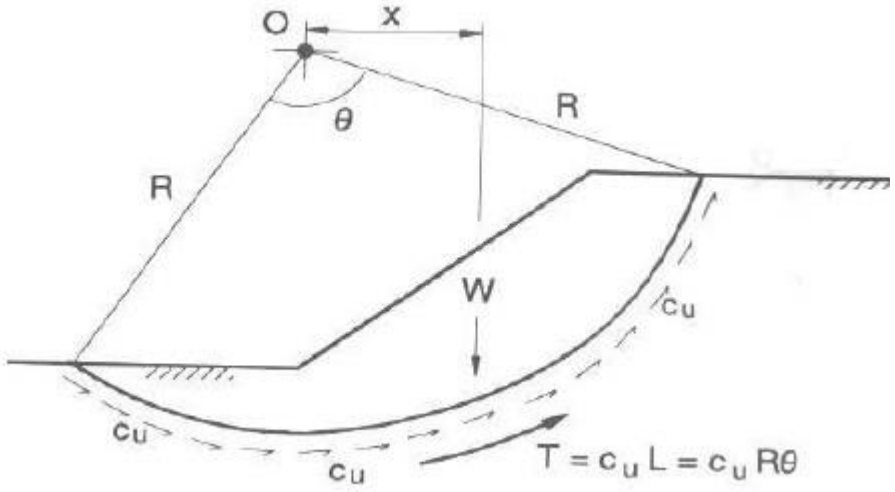

Figure 3. Swedish Circle (Abramson 2002)

$$F = \frac{c_u L R}{W x} \qquad \text{Equation 1}$$

where: c_u is undrained cohesion

L is length of circular arc

R is surface's radius

W is weight of failure mass

x is horizontal distance between circle center and the center of the mass of the soil

As it is obvious, the main need in this method is to assume the failure circle (to determine the location of the slip surface) and the method suggest you to use trial and error to find the critical circle.

2.2.A.1.1.2 The Friction Circle Procedure

This method has been developed to analyze homogenous soils with a $\varphi > 0$. In this method, the resultant shear strength (normal and frictional components) mobilizes

along the failure surface to form a tangent to a circle, called friction circle, with a radius of R_f. Figure 4 shows the friction circle. R_f can be found by getting help from the following equation:

$$R_f = R \sin \varphi_m \qquad \text{Equation 2}$$

where R is the failure circle's radius,

φ_m , is the mobilized friction angle, can be found using

$$\varphi_m = \tan^{-1} \frac{\varphi}{F_\varphi} \qquad \text{Equation 3}$$

Where F_φ is the factor of safety against the frictional resistance (Abramson, 2002).

This method uses a recursive calculation; Abramson et al. (1996) suggested the following procedure to determine the factor of safety.

1) Determine the weight of the slip, W.
2) Determine direction and greatness of the resulting pore water pressure, U.
3) Determine perpendicular distance to the line of action of C_m, R_c , which can be located using

$$R_c = \frac{L_{arc}}{L_{chord}} . R \qquad \text{Equation 4}$$

where The lengths are the lengths of the circular arc and chord defining the failure mass.

4) Calculate effective weight resultant, W', from forces W and U. And its intersection with the line of action of C_m at A.
5) Adopt a value for F_φ
6) Compute φ_m
7) Draw the friction angle using R_f
8) Draw the force polygon with w', appropriately inclined, and passing through point A.
9) Draw the direction of P, the resultant of normal and frictional force tangential to the friction circle.
10) Draw direction of C_m, according to the inclination of the chord linking the end points of the circular failure surface.
11) The closed polygon will then provide the value of C_m.
12) By means of this value of C_m , compute F_c:

$$F_c = \frac{cL_{chord}}{C_m} \qquad \text{Equation 5}$$

13) Repeat steps 5 to 12 until $F_c \approx F_\varphi$.

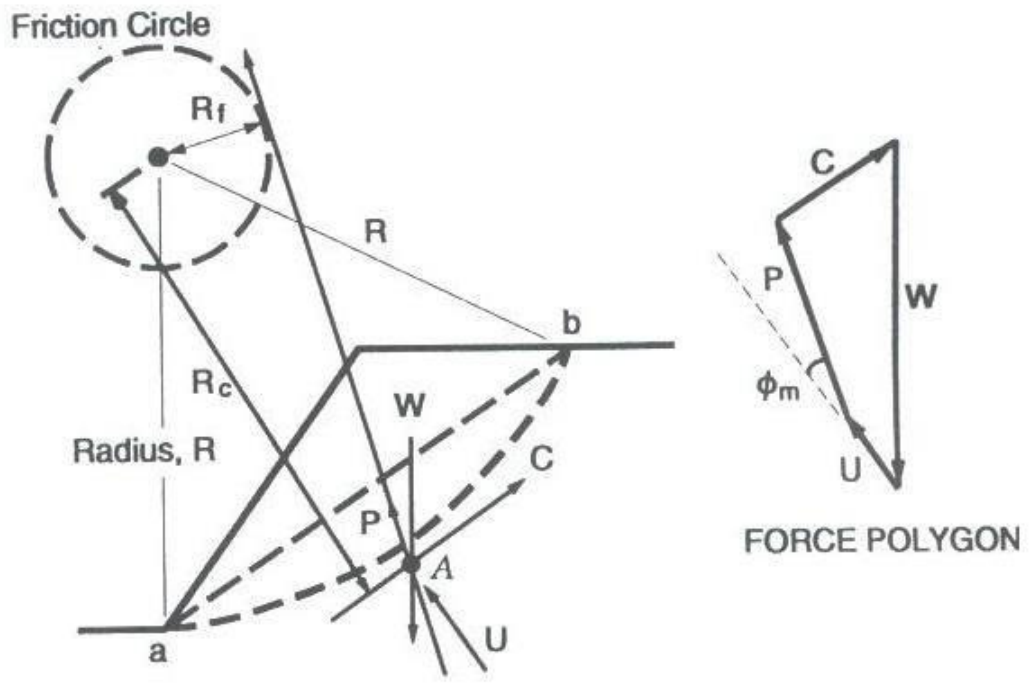

Figure 4. Friction Circle Method (Abramson 2002)

As it is clear in this method, knowing the failure surface is an imposition.

2.2.A.1.2 Non-Circular Method

2.2.A.1.2.1 Log-Spiral Procedure

In this technique, the slip surface will be presumed to have a logarithmic shape, using following formula for its radius:

$$r = r_0 e^{\theta \tan \varphi_d} \qquad \text{Equation 6}$$

where r_0 is the initial radius,

θ is the angle between r and r_0, and

φ_d is developed friction angle

The shear and normal stresses along the slip could be calculated using following equations:

$$\tau = \frac{c}{F} + \sigma \frac{\tan \varphi}{F} \qquad \text{Equation 7}$$

$$\tau = c_d + \sigma \tan \varphi_d \qquad \text{Equation 8}$$

where c and φ are the shear strength parameters,

c_d and φ_d are the developed cohesion and friction angle, and

F is the factor of safety.

By assuming this specific shape shown in Figure 5, normal stress and the frictional stress will pass through the spiral center, hence they will produce no moment about the center. So the only moment producing forces will be weight of the soil and the developed cohesion.

Since the developed friction,φ_d is present in the r formula. This method is also a recursive procedure, hence several trials should be done to obtain a factor of safety which satisfies the following equation (J Michael Duncan & Wright, 2005).

$$F = \frac{c}{c_d} = \frac{\tan \varphi}{\tan \varphi_d} \qquad \text{Equation 9}$$

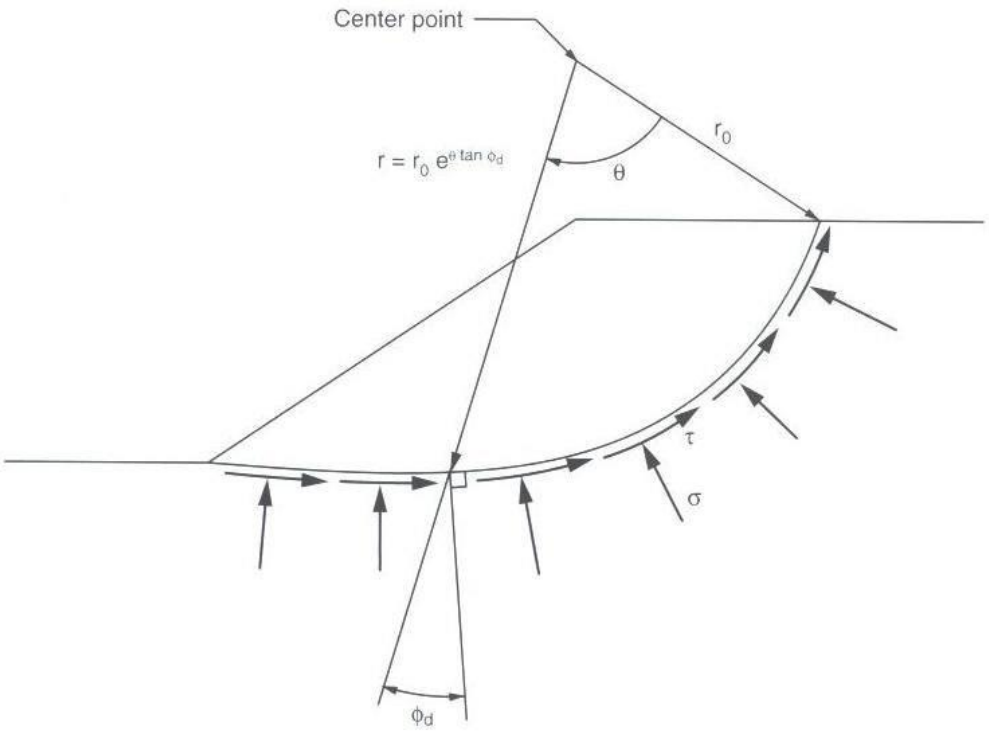

Figure 5. Log-Spiral Method (Duncan and Wright 2005)

In this method, having known the failure surface is important because the procedure starts with knowing an R_0 and a center for the spiral.

2.2.A.1.3 Methods of slices

In the methods of slices, the mass of soil over the failure area will be divided into several vertical slices and the equilibrium of each of them is studied singly. However, breaking up a statically in-determined problem into several pieces does not make it statically determined; hence an assumption is needed to make them solvable. By classifying these assumptions, these methods will be distinguished.

The important issue here is again, in these methods knowing the failure surface is important since these methods are based on dividing the soil mass above the slip. Numbers of more useful methods from this group will be discussed here.

2.2.A.1.3.1 Ordinary method of slices

This technique (a.k.a. "Swedish Circle Technique" and "Fellenius' Technique"), assumes that the resultant of the inter-slices forces in each vertical slice is parallel to its base hence they are ignored and only the moment equilibrium is satisfied. Studies (Whitman & Bailey, 1967) have shown that FSs calculated with this method is sometimes as much as 60 percent conservative, comparing to more exact methods, hence this technique is not being hired much nowadays.

For the slice shown in the Figure 6, the Mohr-Coulomb failure criterion is:

$$s = c' + (\sigma - u)\tan\varphi' \qquad \text{Equation 10}$$

Using a factor of safety, F, $t = s/F$, $P = s \times l$ and $T = t \times l$, the equation will be:

$$T = \frac{1}{F}(c'l + (p - ul)\tan\varphi' \qquad \text{Equation 11}$$

Having interslice forces neglected, makes the normal forces on the base of slice as:

$$P = w\cos\alpha \qquad \text{Equation 12}$$

where w is the slice's weight and

α is the angle between the global horizontal and center of the slice base's tangent.

Moment about the center of the slope failure shape will be:

$$\sum W\ R\ \sin\alpha = \sum T\ R \qquad \text{Equation 13}$$

Therefore:

$$FoS = \frac{\sum(c'l+(w\cos\alpha - ul).\tan\varphi')}{\sum W\ \sin\alpha} \qquad \text{Equation 14}$$

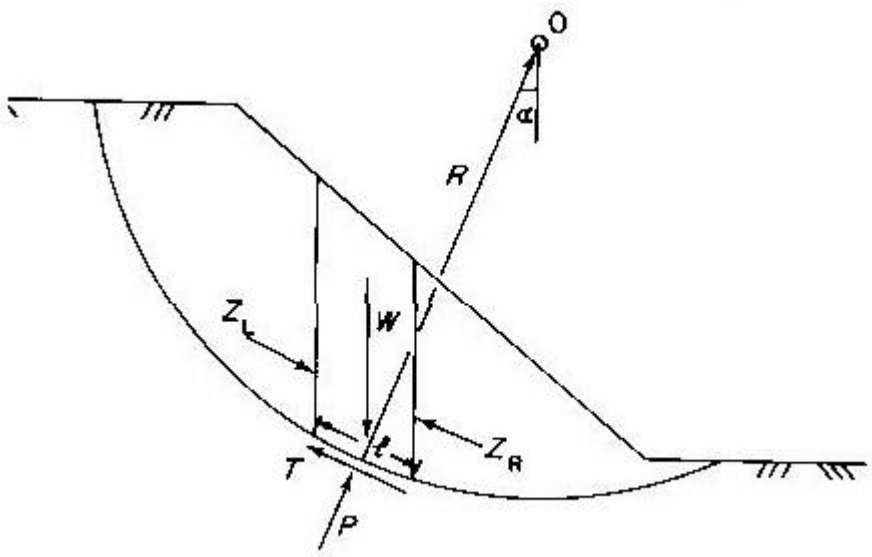

Figure 6. Ordinary Method of Slices (Anderson and Richards 1987)

As it is shown in the procedure, to compute the factor of safety hiring this method, knowing the failure surface is again necessarily (Anderson & Richards, 1987).

2.2.A.1.3.2 Simplified Bishop Method

This method finds the factor of safety by assuming that the failure happens by rotation of a circular mass of soil as demonstrated in Figure 7. While the forces between the slices are considered horizontal, no active shear stress is between them. The normal force of each slice, P, is presumed to act on each base's center. This force may be computed using Equation 15.

$$P = \frac{[W - {}^{1}/_{F}(c'l \sin\alpha - ul \tan\varphi' \sin\alpha]}{m_\alpha} \qquad \text{Equation 15}$$

where:

$$m_\alpha = \cos\alpha + \frac{(\sin\alpha \tan\varphi')}{F} \qquad \text{Equation 16}$$

By taking moment about the circle's center:

$$F = \frac{\sum\left[\frac{c'l\cos\alpha + (w - ul\cos\alpha)\tan\varphi'}{\cos\alpha + \frac{\sin\alpha\tan\varphi'}{F}}\right]}{\sum W \sin\alpha} \qquad \text{Equation 17}$$

As the above formula shows, having F on both sides, this forces us to solve it iteratively. This procedure is usually quick, and gives a relatively accurate answer, with 5 percent difference to FEM methods, hence it is suitable for hand calculations (Anderson & Richards, 1987).

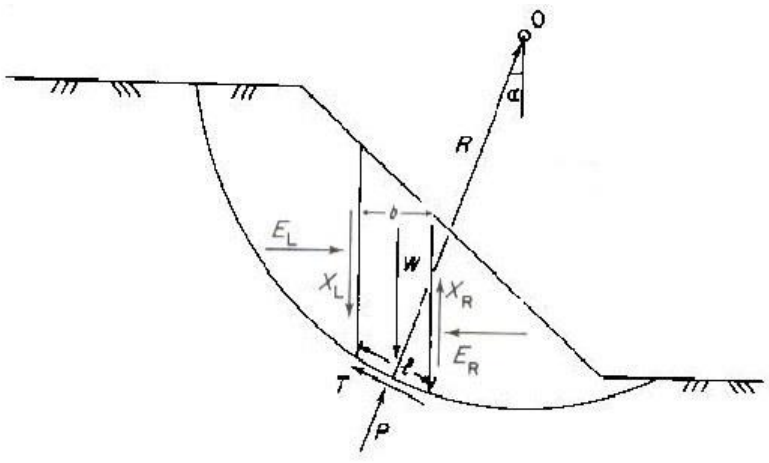

Figure 7. Simplified Bishop Method (Anderson and Richards 1987)

Like the other methods, it needs to assign the failure surface in the beginning.

2.2.A.1.3.3 Spencer's Method

Although Spencer's method was originally presented for circular failure surface, it has been easily extended for non-circular slips by assuming a frictional center of rotation. By assuming parallel interslices forces, they will have same inclination:

$$\tan\theta = \frac{X_l}{E_l} = \frac{X_R}{E_R} \qquad \text{Equation 18}$$

where θ is the angle of the interslices forces from the horizontal.

By summing the forces perpendicular to the interslices forces, the normal force on the base of the slices will be:

$$P = \frac{W-(E_R-E_l)\tan\theta-{}^{1}/_{F}(c'l\sin\alpha-ul\tan\varphi'\sin\alpha)}{m_\alpha} \qquad \text{Equation 19}$$

where

$$m_\alpha = \cos\alpha\left(1+\tan\alpha\,{}^{\tan\varphi'}/_{F}\right) \qquad \text{Equation 20}$$

By considering overall force and moment equilibrium in Figure 8, two different factors of safety will be derived; this is because of the total assumptions that have been made the problem over specified.

The factor of safety from moment equilibrium, by taking moment about O:

$$\sum WR\sin\alpha = \sum TR \qquad \text{Equation 21}$$

where

$$T = \frac{1}{F}(c'l + (p - ul)\tan\varphi' \quad \text{Equation 22}$$

$$F_m = \frac{\sum(c'l+(p-ul)\tan\varphi'}{\sum W \sin\alpha} \quad \text{Equation 23}$$

The factor of safety from force equilibrium, by considering$\sum F_H = 0$:

$$T\cos\alpha - P\sin\alpha + E_R - E_L = 0 \quad \text{Equation 24}$$

$$\sum E_R - E_L = \sum P\ \sin\alpha - {}^{1}/_{F_f}\sum(c'l + (P - ul)\tan\varphi')\ \cos\alpha \quad \text{Equation 25}$$

Using the Spencer's assumption ($\tan\theta = \frac{X_l}{E_l} = cte$) and $\sum X_R - X_L = 0$, in absence of surface loading:

$$F_f = \frac{\sum(c'l+(P-ul)\tan\varphi')\sec\alpha}{\sum(W-(X_R-X_L))\ \tan\alpha} \quad \text{Equation 26}$$

Trial and error method should be done to determine the factor of safety which satisfies both of the equations. Spencer examined this procedure and showed that at a proper angle (for interslices forces), both of the factors of safety values obtained from both equations will become equal, and that value will be considered as the factor of safety (Spencer, 1967).

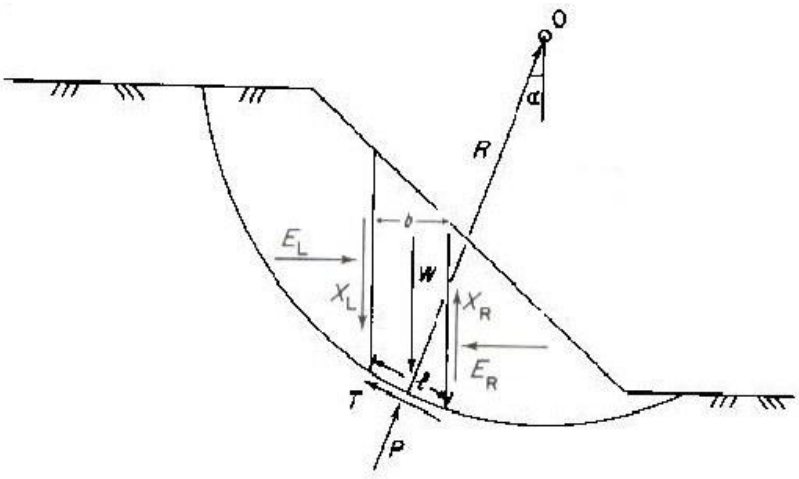

Figure 8. Spencer's Method (Anderson and Richards 1987)

And again in this method, having the correct failure surface is important.

2.2.A.2 Three-Dimensional methods

These methods are based on considering a 3D shape for the failure surface, and are useful for geometrically more complex slopes or while the material of the slope is highly inhomogeneous or anisotropic.

Like the two-dimensional methods, these methods will solve the problems by making assumptions to either decrease the numbers of unknowns or adding additional equations or in some cases both to achieve a statically determined situation.

Generally speaking, most of these methods are an extension from the two-dimensional methods.

Although in this research, the author is not going to discuss them, some of the more useful methods will be introduce by name. For more information about them, please refer to the references given in the reference section of this thesis.

Table 1. Methods of Analyzing 3D Slope Stability (Duncan 1996)

Author	Method
(Anagnosti, 1969)	Extended Morgenston and Price
(Baligh & Azzouz, 1975)	Extended circular arc
(Giger & Krizek, 1976)	Upper bound theory of perfect plasticity
(Baligh, Azzouz, & Ladd, 1977)	Extended circular arc
(Hovland, 1979)	Extended Ordinary method of slices
(A. Azzouz, Baligh, & Ladd, 1981)	Extended Swedish Circle
(Chen & Chameau, 1983)	Extended Spencer
(A. S. Azzouz & Baligh, 1983)	Extended Swedish Circle
(D Leshchinsky, Baker, & Silver, 1985)	Limit equilibrium and variational analysis
(Keizo Ugai, 1985)	Limit equilibrium and variational analysis
(Dov Leshchinsky & Baker, 1986)	Limit equilibrium and variational analysis
(R Baker & Leshchinsky, 1987)	Limit equilibrium and variational analysis
(Cavoundis, 1987)	Limit equilibrium
(Hungr, 1987)	Extended Bishop's modified
(Gens, Hutchinson, & Cavounidis, 1988)	Extended Swedish circle
(K Ugai, 1988)	Extended ordinary technique of slices, Janbu and Spencer, modified Bishop's
(Xing, 1988)	LEM
(Michalowski, 1989)	Kinematical theorem of limit plasticity
(Seed, Mitchell, & Seed, 1990)	Ad hoc 2D and 3D
(Dov Leshchinsky & Huang, 1992)	Limit equilibrium and variational analysis

2.2.B Finite Element Methods

Finite element methods use a similar failure mechanism to LEM and the main difference between them is, by using the power of finite element, these methods do not need the simplifying assumptions.

This method, in general, firstly proposes a slip failure, and then the factor of safety, which is introduced as the ratio of available resistance forces to deriving forces, will be calculated.

There are two more useful finite element methods; Strength reduction method and gravity increase method.

2.2.B.1 Gravity Increase Method

In this technique, gravity forces will be increased bit by bit until the slope fails. This value will be the gravity of fail, g_f.

Factor of safety will be the ratio between gravitational acceleration at failure and the actual gravitational acceleration. (Swan & Seo, 1999)

$$FS = \frac{g_f}{g} \qquad \text{Equation 27}$$

where: g_f : Increased gravity at failure level

g: Initial gravity

2.2.B.2 Strength Reduction Method, SRM

In SRM, the strength parameters of soil will be decreased until the slope fails and the factor of safety will be the ratio between the actual strength parameters of the soil and the critical parameters.

The definition of factor of safety in SRM is exactly same as in LEM (Griffiths & Lane, 1999)

The gravity increasing technique is more often hired to study the stability of slopes in the construction phase, since its results are more reliable, while SRM is more useful to study the existing slopes. (Matsui & San, 1992)

2.2.C Difference between LE and FE methods

Although LE methods are more easy to use, less time consuming, and can be used for hand calculations, they have some limitations to compute forces especially in parts of the slope where the localized stress concentration is high and due to this limitations the factor of safety in LE methods become slightly higher(Aryal, 2008; Bojorque, De Roeck, & Maertens, 2008; Khabbaz, 2012), in addition some researchers believe that FE methods are more powerful specially for cases with complex conditions (James Michael Duncan, 1996).

On the other hand, number of researchers believe that the results of LE and FE methods are almost equal (Azadmanesh & Arafati, 2012; Stephen Gailord Wright, 1969; Stephen G Wright, Kulhawy, & Duncan, 1973)although Cheng believes that this agreement is unless the internal friction angle is more than zero (Y. M. Cheng, T. Lansivaara, & W. B. Wei, 2007).

Even though both LE and FE methods have their own advantages and disadvantages, the use of neither of them is superior to the other one in routine analysis (Y. Cheng, T. Lansivaara, & W. Wei, 2007).

2.3 Soil Slope Failure Surface Searching Methods

As it was shown in the previous section, there are lots of different methods to analyze the stability of soil slopes, either man-made or natural slopes. Each of them guides us to a different factor of safety. Some of them are more accurate, such as FEMs, some are conservative, like ordinary method of slices. But these differences are only for one slip failure, which should be the critical one. The procedure to find this critical failure surface itself has numerous methods too. Some of them are so complicated while some others are less, but mostly they just can be done using computers and they are very difficult to be used for hand calculations. Also for complicated problems (with a thin soft layer of soil), the factor of safety is very sensitive to the precise location of the critical solution and differences between different global optimization methods are found to be large (Cheng, Li, Lansivaara, Chi, & Sun, 2008).

Until now, most of these methods are based on trial and error methods to optimize this procedure. Different optimization methods, such as genetic algorithm (GA), annealing, and etc., have developed different search methods.

In this section, some of more recent methods will be discussed.

2.3.1 Simulated Annealing Method

In this method, the optimization has been done by adopting annealing method to achieve the global minimum factor of safety. It is based on two user-defined first points, (which are defined completely following) and then another upper bounds and all the rest will be produced by the given algorithm.

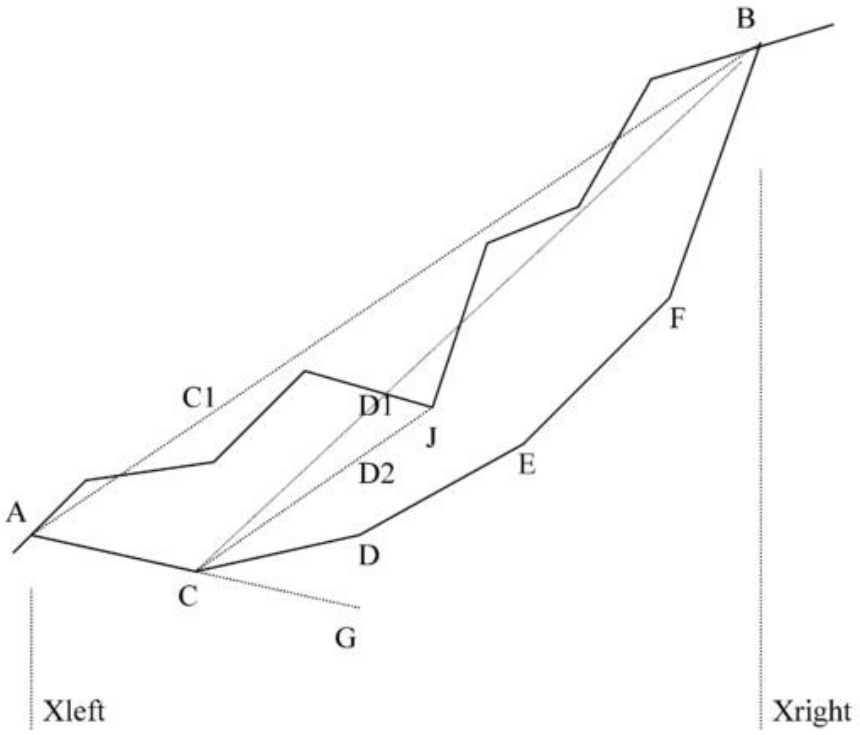

Figure 9. Typical Failure Surface (Cheng 2003)

For a typical failure surface ACDEFB as shown in the Figure 9, the coordinates of the two exit ends, A and B, are taken as control variables, and the upper and lower bound of these variables will be specified by user. The rest will be done by the following algorithm designed by (Cheng, 2003):

1. The x-ordinate of the interior points, C, D, E, and F, will be calculated by uniform division of the horizontal distance between A and B.
2. The y-ordinate if the C1, which is a point located over C, will be the minimum of:
    a. Y-ordinate of the ground profile under the C point.
    b. Y-ordinate of the point on the line joining A and B, exactly under (or above) the C point

C1 will be the upper bound of the y-ordinate of the first slice; its lower bound is set by the methods author as C1-AB/4

3. C is defined by choosing a y-ordinate in the given domain. Draw a line from A to C and extend it to x-ordinate of D, it will be G, the lower bound of the point D. The upper bound for D, D1, will be determined same as C1.
4. Repeat step 3 for remaining points.

In this method, the author claims that using this technique, the failure surface can be located in 3 to 5 minutes with a PII 300 computer, which is quiet useful for computer programs (Cheng, 2003).

For more information regarding this method, please refer to the original paper.

2.3.2 Simple Genetic Algorithm

This method presents a simple calculation method based on the Morgenstern-Price's slope stability analysis method for non-circular failure surfaces with pseudo-static earthquake loading (McCombie & Wilkinson, 2002), this method is a simplified version of genetic algorithm (Sengupta & Upadhyay, 2009).

Simple genetic algorithm (SGA) has been used in this method in order to find the critical non-circular slip surface. Figure below (Figure 10) shows the algorithm to find the slip using this method (Zolfaghari et al., 2005).

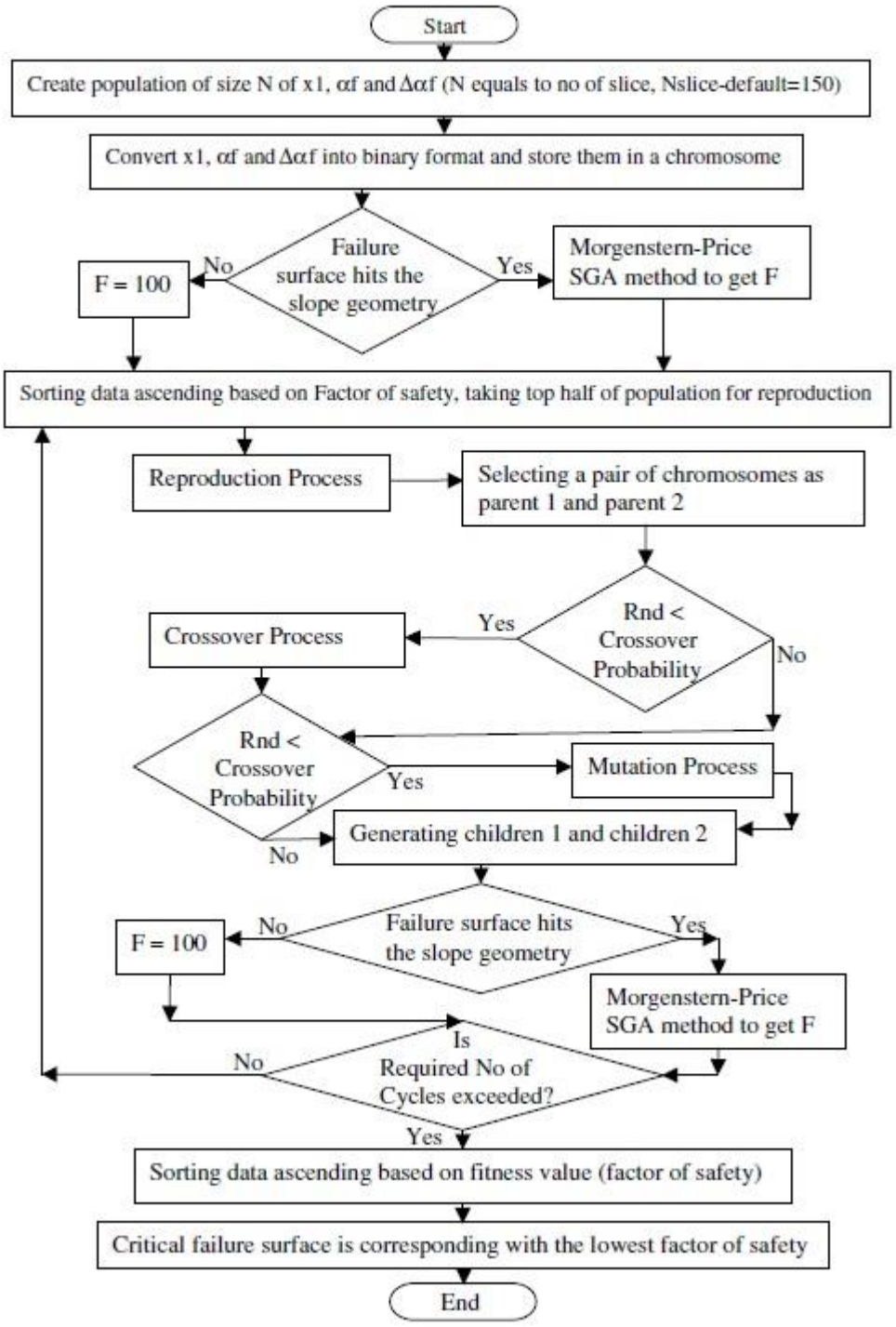

Figure 10. Simple Genetic Algorithm (Zolfaghari et al., 2005)

2.3.3 Leapfrog Algorithm Method

This searching method is based on the Janbu's and Spencer's techniques of slope stability analysis. The reason that the authors used these methods for their study is that none of them needs any prior geometry assumption, and there is no limitation regarding initiation of termination points of the slip in these methods. This makes the method able to result a general formulation for slip surface.

This method first presents an algorithm to find the factor of safety as it is described below:

1. Initialization: Set the counter $j := 1$, propose the parameters t_{max}; n_1; k_{max}; l_{max} and x_{beg}. Here, x_{beg} signifies the maximum random starting value for $x_3, x_4, x_5, \ldots, x_{nk+1}$, t_{max} the number of global phase iterations, n_1 the starting number of slices, k_{max} the maximum number of adaptive slicing circles in the global stage and l_{max} the maximum number of adaptive slicing circles in the local stage.

2. Global Optimization phase:
   (a) Sampling steps: Set the counter $k := 1$ and start with n_k slices and randomly produce $x_k^j \in D$, i.e. choose x_1 and x_2 randomly within the slope geometry and produce random values for $x_3, x_4, x_5, \ldots, x_{nk+1}$, t_{max} between 0 and depth x_{beg}.
   (b) Minimization steps: Starting at x_k^j , attempt to minimize F in a global sense by any optimization procedure, viz. find and note some low function value $\tilde{F}_k^j \leftrightarrow \tilde{x}_k^j$

(c) Termination check: If $k = k_{max}$ or $\tilde{F}_k^j \geq 10$ go to step 3, else continue.

(d) Double number of slices: Set $k := k + 1$, double the number of slices ($n_k := 2n_{k-1}$) and determine the new starting vector x_k^j from $\tilde{x}_{k-1}^j$. Go to step 2(b).

3. Global Termination: If $j = t_{max}$ goto step 4, else $j := j + 1$ and goto step 2.

4. Local improvement stage:

(a) Initialization: Set the counter $l := 2$ and define the starting vector $\tilde{x}_1$ for the local improvement stage from $\tilde{x}_k^j$ which agrees to minimum noted $\tilde{F}_k^j$ for $j = 1, 2, \ldots, \tilde{n}$. Set $\widehat{F_1} = \tilde{F}_k^j$ and the number of slices are $n_1 := 2n_k^j$.

(b) Minimization steps: Starting at $\bar{x}_1$ try to minimize F in a local sense by any optimization procedure, viz. find and note some low function value $\widehat{F_l} \leftrightarrow \widehat{x_l}$.

(c) Termination check: If $l = l_{max}$ or $\widehat{F_l} > \widehat{F_{l-1}}$ go to step 5, else continue.

(d) Double number of slices: Set $l := l + 1$, double the number of slices ($n_l := 2n_{l-1}$) and define the new starting vector $\bar{x}_l$ from $\bar{x}_{l-1}$. Goto step 4 (b).

5. Slope Stability Termination: Take the lowest recorded $\widehat{F_l}$ for $l = 1, 2, 3, \ldots$ as factor of safety. STOP

Then the author claims, after testing a number of optimization methods, the most efficient procedure proved to be the Leapfrog algorithm (Bolton et al., 2003).

2.3.4 Other methods

From other methods, "Particle swarm optimization algorithm" (Cheng, Li, Chi, & Wei, 2007), and "Monte Carlo techniques" (Malkawi, Hassan, & Sarma, 2001) can be counted which would not be considered in this thesis.

2.4 Potential Slope Failure Surface and Soil Strength Parameters

The effect of soil strength parameters on factor of safety has been studied for numerous times, but their effect on slip surface has seldom been considered.

One of very few papers (Lin & Cao, 2011), talks about the relation between these parameters and potential slip surface and how they affect the failure surface.

This paper presents a function of cohesion c, internal friction angle φ, unit weightγ, and height of the slope h as:

$$\lambda = c/(\gamma\, h\, \tan\varphi) \qquad \text{Equation 28}$$

The paper discusses that whenever the Lambda value (λ) remains constant, the failure surface remains the same, this is in line with an earlier study, (Jiang & Yamagami, 2008), which indicates there is a unique relation between $c/\tan\varphi$ and slip surface. Moreover the greater λ indicates a more deep failure slip and smaller λ makes the failure surface come closer to the slope surface (Lin & Cao, 2012).

Chapter 3

METHODS AND SOFTWARES USED IN THE STUDY

3.1 Introduction

In this chapter, methods and software programs that are going to be used in this study will be introduced, and briefly discussed.

3.2 Methodology

As it has been discussed in the previous chapters, for each slope, there are deriving forces and resisting forces which should be considered. Deriving forces are mostly due to the weight of the soil block that is in a direct relation with the unit weight of the soil, and resisting forces are mostly due to cohesion and internal friction angle of the soil.

In failure surface determination, each one of the aforementioned parameters has its own effect on slope surface. For example, in Swedish Circle method, when the diameter of the cylindrical failure shape is increased, the weight of the failure soil and the perimeter of the shape are increased, meaning more friction and cohesion are developed. Thus, both the deriving and resisting forces are getting bigger, and due to the fact that, the factor of safety has a direct relation with resisting forces and indirect relation with the deriving forces. That means the factor of safety increases by increasing resisting forces, and decreases because of the increase in the deriving forces.

In first part of this study, the effect of unit weight γ, cohesion c, and the internal friction angle ϕ of the soil will be studied on the factor of safety and the location of the failure surface will be determined by using the same soil parameters.

In the second part of the study, the sufficient numbers of slopes will be modeled with varying soil shear strength parameters, unit weights, and slope geometry in order to create a database of failure surfaces regarding these slope parameters.

Finally, a multi-variable regression will be carried out in the database created in the second part of the study, to find a numerical formula to locate the failure surface.

In the first two parts, the study will be performed by using the educational license of the last version of the GEO5 software, Slope-Stability v16.

Since unreasonable results may be obtained from all the commercial programs (Cheng, 2008), in this study, in order to check and control the accuracy of the results obtained from GEO5 software program, a study will be conducted to compare the findings between the results obtained from GEO5 and the other software programs. In the study, the models will be re-analyzed by using student license of Geo-Studio 2012 software, SLOPE/W.

A random selection of the generated models, will be re-analyzed using FLAC/Slope software for factor of safety, since this software does not report the failure surface.

The output data of the failure surface of the models will be used to draw the slope in the latest version of Automatic Computer-Aided Design (AutoCAD) software (2014

(I.18.0.0)) from the Autodesk Company to measure the length of the failure arc and locate the slip surface entry point by measuring its distance to the slope edge.

The result of analyzing each model will be entered and stored into latest version of Microsoft Excel (2013 (15.0.4433.1506)) a spreadsheet program under the Microsoft Office package. After this step, using this software, different figures will be generated. In the last step of this study, using International Business Machine (IBM)'s software called Statistical Package for the Social Sciences (SPSS), a regression will be carried out in order to find a relation between input and output data.

3.3 Materials

3.3.1 Soil

In this study, more than 70 soil types with different strength parameters have been used to be analyzed. In order to generate models with enough accuracy in finding the relation between the soil strength parameters and the failure surface different soil types with small changes in soil strength parameters were selected and analyzed.

The range of soil strength parameters chosen for the study can be seen in Table 2.

Table 2. Soil Strength Parameters

No	Soil Strength Parameter	Range
1	Unit Weight	15~31 kN/m^3
2	Internal Friction Angle	15~32 °
3	Cohesion	15~32 kPa

3.3.2 Water Level

In this study, due to limitation of time, effect of water content has not been studied. Omitting its effect has been done by assuming the water level being far below the slope level. Thus the soil has been assumed to be dry.

3.4 Software and Programs

3.4.1 GEO5

In this study, a student version of the "Slope Stability" software from the GEO5 software package has been used. In order to minimize the possible bugs and problems of the software, its last version (16.3) has been hired.

In the first step, for each of the models, using the "Interface" tab, and the "Add" button, coordinates of the slope will be entered as shown in Figure 11.

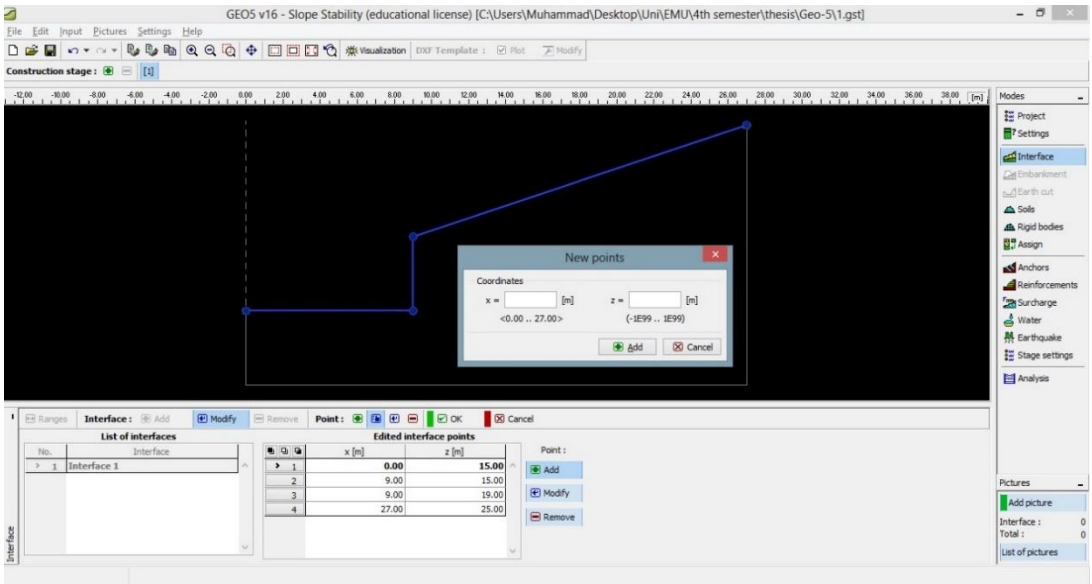

Figure 11. GEO5 Interface

Next step will be entering the properties of the soil using “Add” button under “Soil” tab as shown in Figure 12 and then assigning it to the slope interface, from the “Assign” tab.

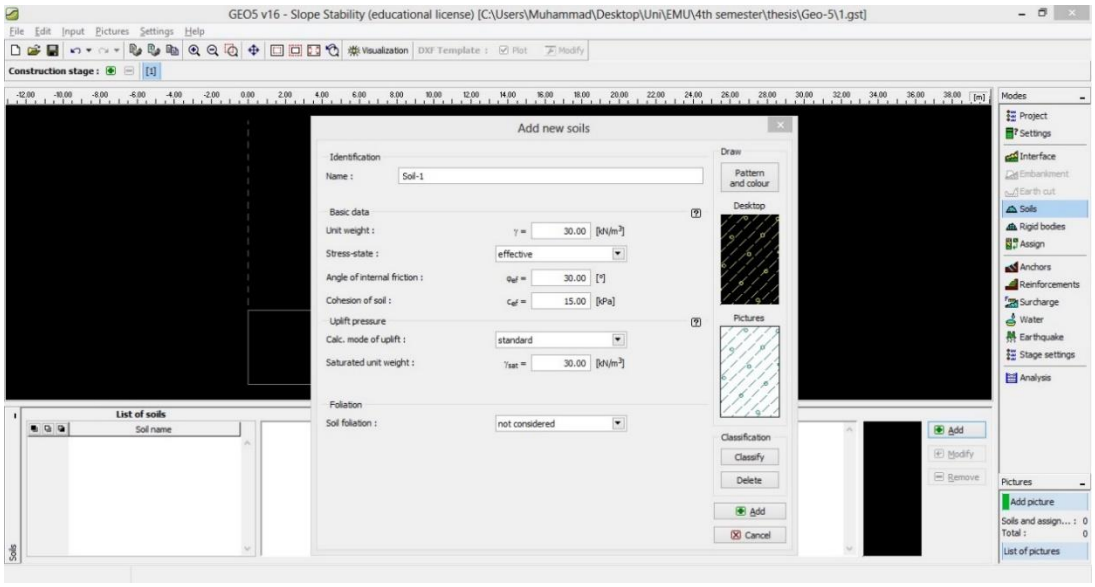

Figure 12. GEO5 Soil Properties

In this step, a first guess for the failure surface will be entered in the “Slip Surface” part under “Analysis” tab, and after using “Bishop” as the method, and setting “Analysis Type” to “Standard” preliminary analysis should be carried out by using “Analyze” button. After that, to analyze the slope and finding the critical failure surface, “Analysis Type” should be changed to “Optimization” and another analysis should be run.

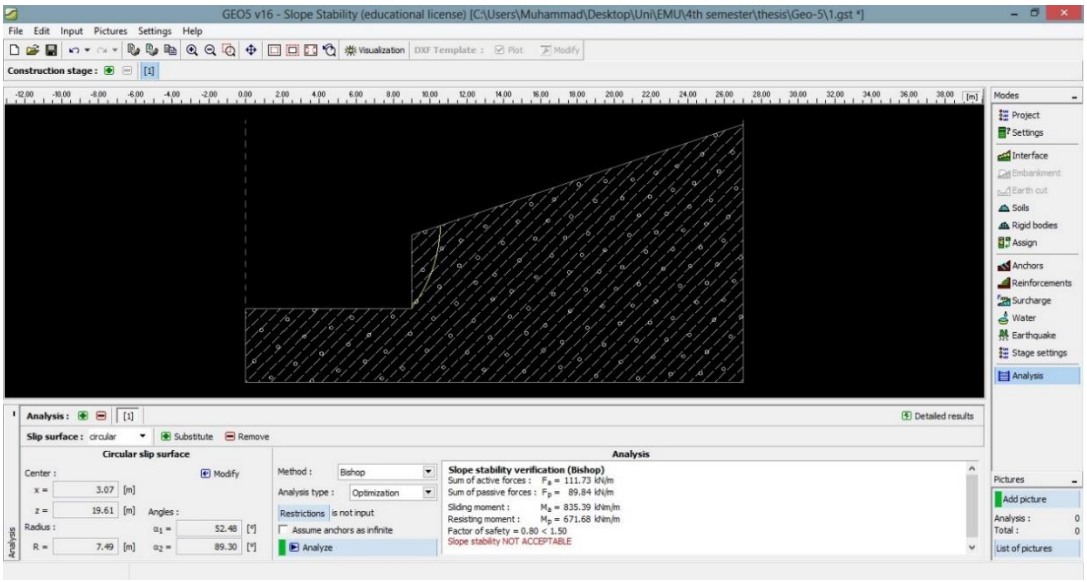

Figure 13. GEO5 Results

From the "Slip Surface" section, details of the critical slip surface and from the "Analysis" section, the minimum factor of safety could be found (Figure 13).

3.4.2 SLOPE/W

In order to check the trustworthiness of the analysis output data, SLOPE/W a sub-program of the Geo-Office software pack which is a professional geotechnical software has been used. For this study, a student license of the latest version of GeoOffice 2012 (Version 8.0.10.6504) has been used.

SLOPE/W is a slope stability analysis software based on Limit Equilibrium, LE and Finite Element, FE methods and supports most of major LE and FE slope analysis methods such as Bishop, Spencer, Janbu, and etc. With the intention of achieving the goal of this research, a simple LE method, Bishop's method, with a circular slip surface with 30 increments for entry and exit range and 30 increments for number of radius will be used. Rest of the settings in the program can be found in Figure 14.

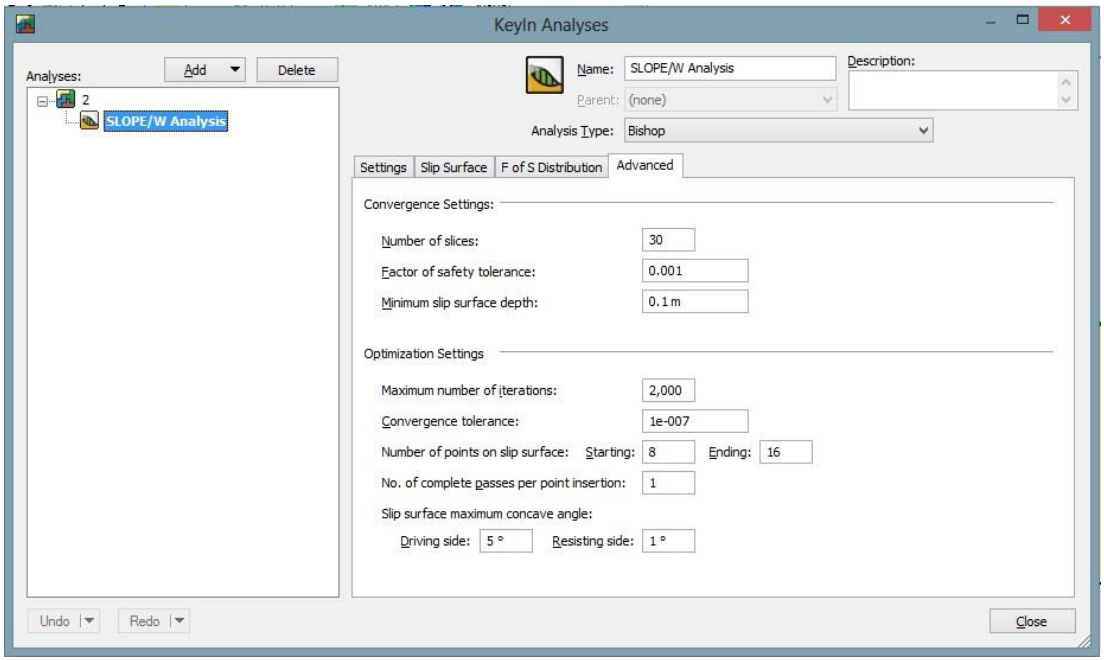

Figure 14. SLOPE/W KeyIn Analyses

For each model, using the drawing tools, the geometry of the slope should be entered. Then by using the "Entry and Exit…" dialogue box, under "Slip Surface" sub-menu, under "KeyIn" menu (Figure 15), the increments for entry and exit range as well as number of radius will be set.

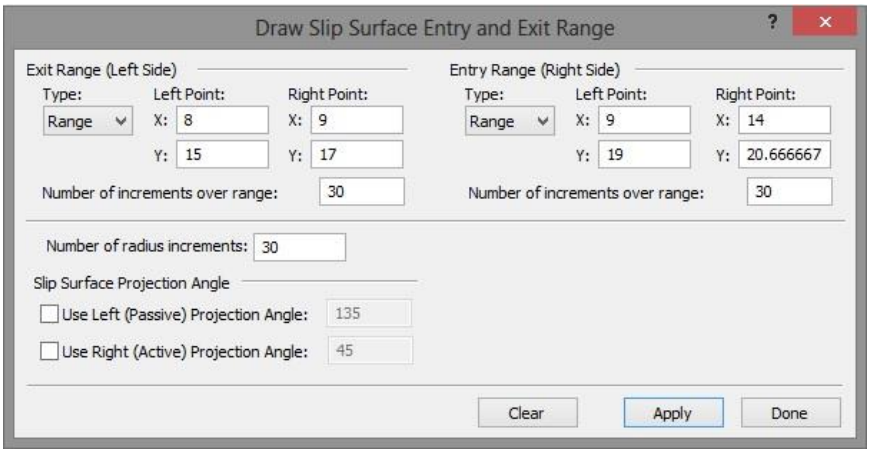

Figure 15. SLOPE/W KeyIn Entry and Exit Range

Then using “Materials” dialogue box under “KeyIn” menu as can be seen in Figure 16, soil parameters will be entered and selected soil will be assigned to the drawing in the software.

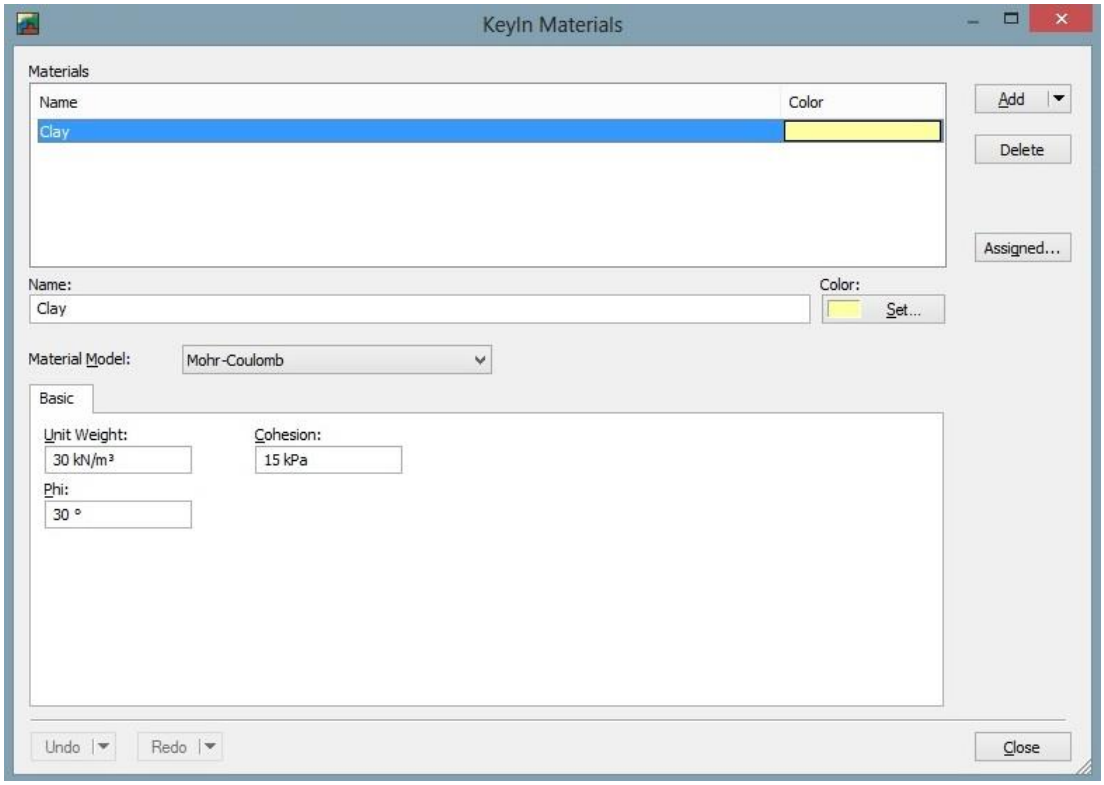

Figure 16. SLOPE/W KeyIn Material

After entering all of the input data into the software by hitting the “Start” button under “Solve Manager”, the program starts to analyze the slope and find the minimum factor of safety and its related failure surface as can be seen in Figure 17.

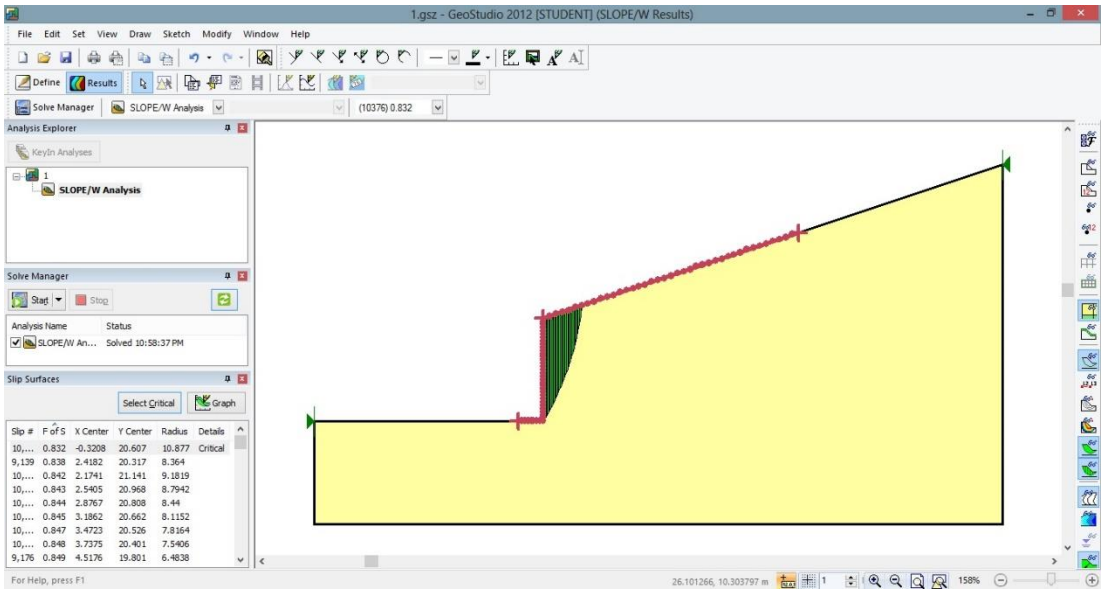

Figure 17. SLOPE/W Results

After the analysis of the slope finishes, under “Slip Surfaces”, the critical failure surface details (coordinates of the center of failure circle and its radius) and its factor of safety can be read. This data will be used in the AutoCAD software to draw the failure surface and measure the length of failure arc.

3.4.3 FLAC/Slope

FLAC/Slope is a sub-program of the Fast Lagrangian Analysis of Continua (FLAC) programs by the ITASCA engineering consulting and software firm. In order to re-check the accuracy of the results of SLOPE/W and GEO5 programs, this software has been used. Since FLAC/Slope does not declare the failure surface, only the factor

of safety has been calculated by this program. Although it should be noted that by using FLAC 3D software and compiling internal programs, the failure surface could then be calculated (Lin & Cao, 2011).

For the purpose of this study, an educational license of the latest version of FLAC/Slope (v2.20.485) has been hired.

In FLAC/Slope, for each of the models, a "Bench-1" slope under "Model" tab will be introduced with the related geometry as shown in Figure 18.

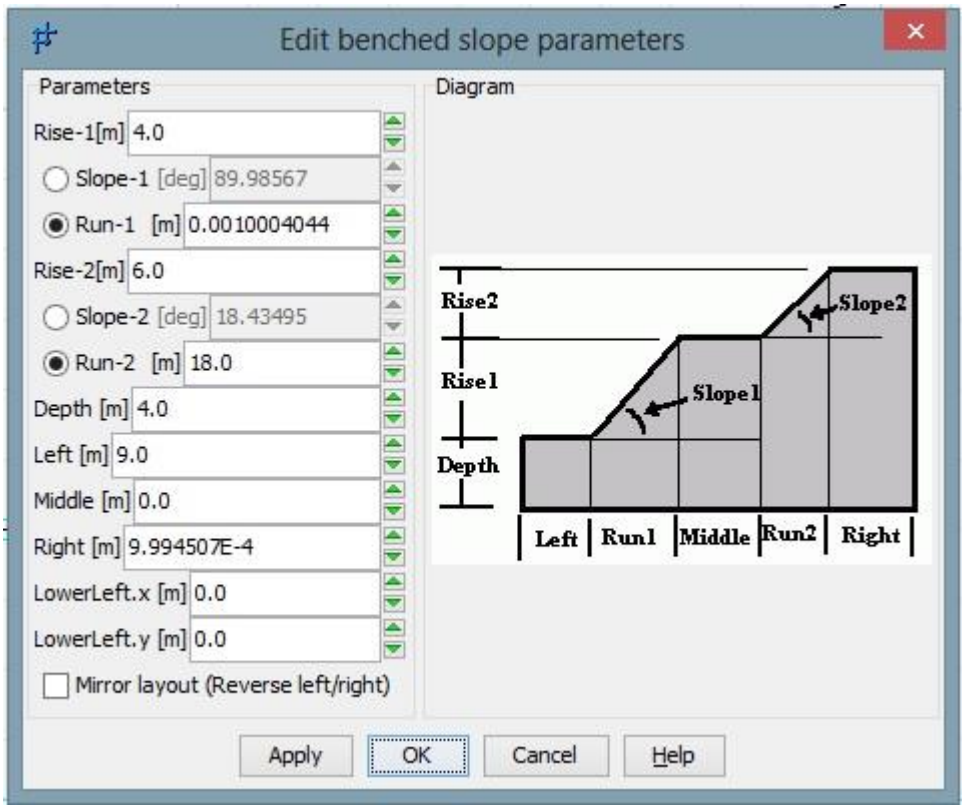

Figure 18. FLAC/Slope Model Parameters

In the next step, by using “Material” window, under “Build” tab, soil properties will be entered in to the program and after that it should be set to the interface by using “Set All” button as shown in Figure 19.

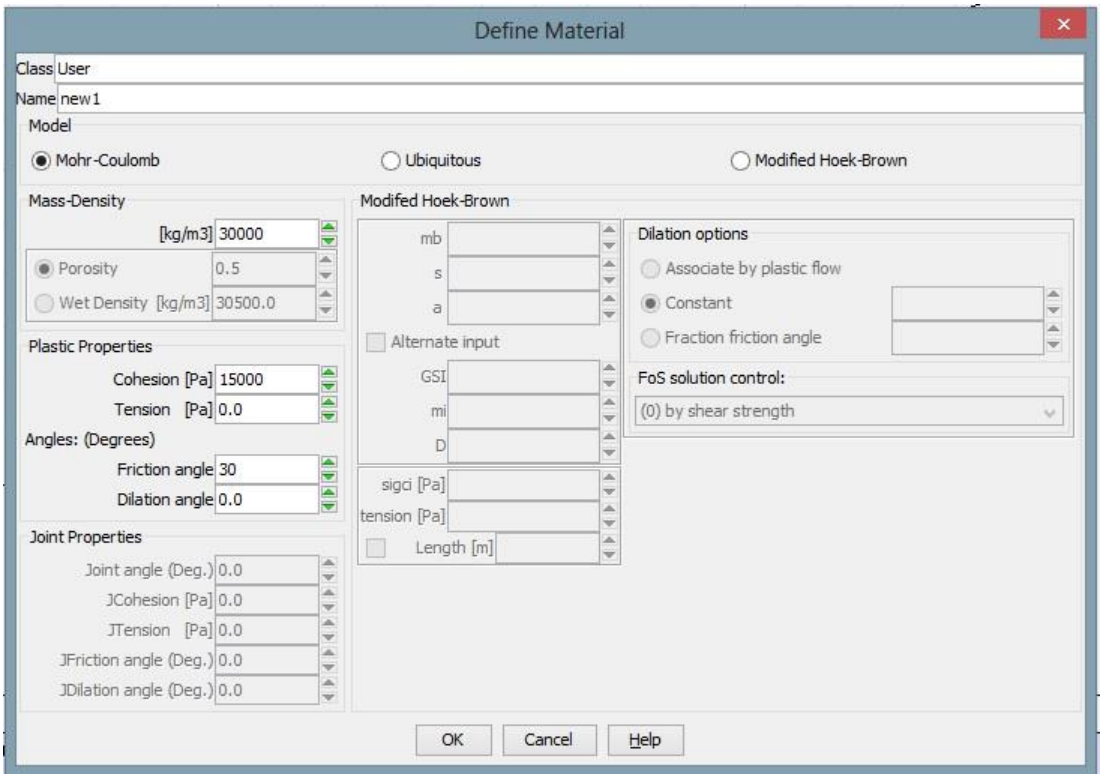

Figure 19. FLAC/Slope Defining Material

After introducing and assigning the materials to the slope, under “Solve” tab, desired type of mesh will be selected between “Coarse”, “Medium”, and “Fine”. Then to find the factor of safety, analyze will be started by clicking on the “SolveFoS” button (Figure 20).

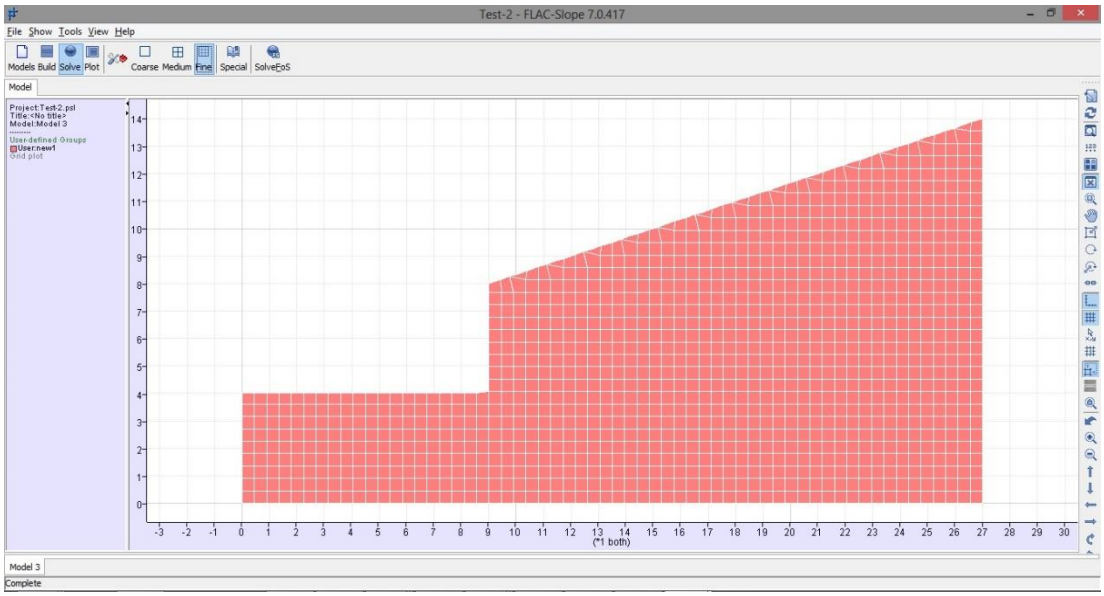

Figure 20. FLAC/Slope Mesh

Since FLAC/Slope does not give the failure surface as an output data, this software will only be used for factory of safety of a random selection of the models.

Chapter 4

RESULT AND DISCUSSION

4.1 Introduction

In this chapter, the influence of each soil strength parameter (c, ϕ, and γ) on the factor of safety and slip surface, has been studied, both separately and together in two stages. For this purpose, in the first part of the study, with the intention of finding out the trend of changes in factor of safety and failure surface, a limited number of models have been studied, and in the second part, in order to find a relatively accurate relation between soil strength parameters and failure surface, sufficient number of models were set, and were examined. After generating and analyzing all of the models, figures have been drawn to show the effects of the variables on the factor of safety and failure surface. Furthermore, the reasons of these different behaviors have been discussed.

4.2 Effect of Soil Strength and Geometry Parameters on Factor of Safety

In this part, so as to study the feasibility of this thesis, three series of modeling have been performed. In each set of models, one of the parameters varied while the other two remained constant. These models have been studied to see if there is any correlation between soil strength parameters and the position of the failure surfaces.

4.2.1 Effect of Unit weight, γ on the factor of safety, FS

To study the effect of unit weight on the factor of safety, the unit weight values varying from 15 to 30 kN/m^3 were chosen while the cohesion and the internal friction angle were taken as 30 kPa and 30 degrees, respectively.

Table 3. Effect of γ on FS

Model No	Unit Weight (kN/m3)	Internal Friction Angle (°)	Cohesion (kPa)	Factor of Safety
1	15	30	30	2.29
2	20	30	30	1.81
3	25	30	30	1.55
4	30	30	30	1.31

The values in Table 3 indicated that as the unit weight of the soil increased, reduction in the factor of safety values was obtained; this reduction is due to the increase in the unit weight which is the main cause of the deriving forces. Increase in the unit weight of the soil caused the slope to be more unstable resulting in a decrease in the factor of safety.

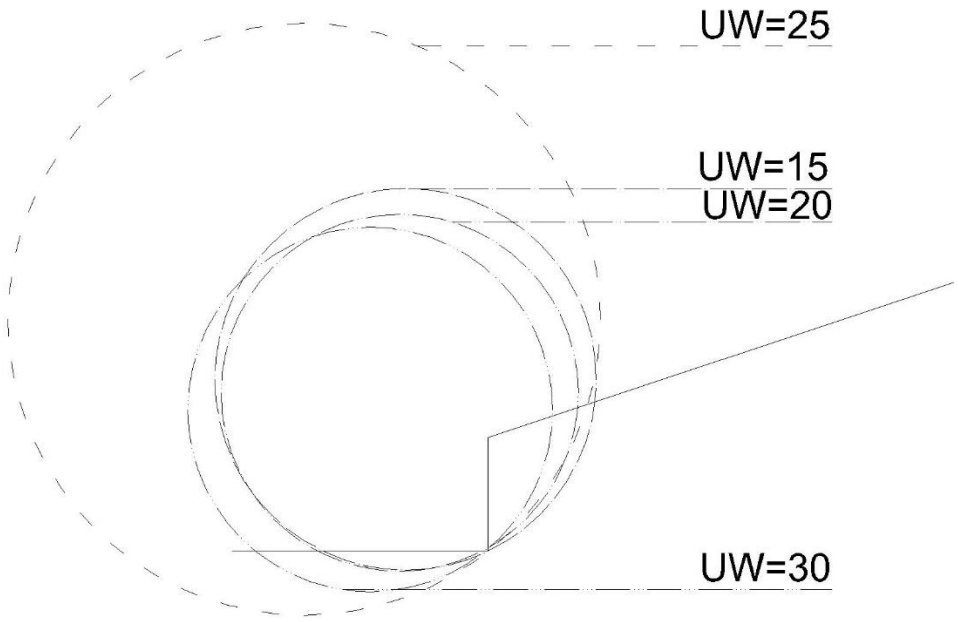

(a)

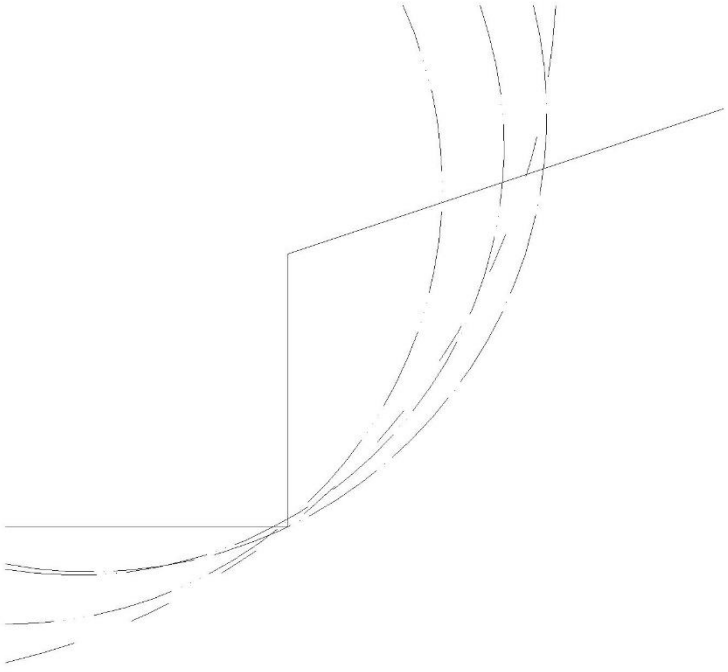

(b)

Figure 21. (a) Effect of γ on Slip Surface, and (b) Exaggerated Part of (a)

Figure 21(a) shows the effect of unit weight on the failure surface (While Figure 21(b) is a zoomed version of (a)). Except for the γ=25 kN/m^3, the other trials follow a logical rule; by increasing the unit weight of the soil, the failure surface is shifted to the left, resulting in smaller failure soil volume and hence reducing the length of the slip surface. Because of the smaller surface for resisting forces (cohesion and friction), less resisting force is activated. Because of these reasons, smaller factor of safety value is achieved.

4.2.2 Effect of Cohesion, c on the Factor of Safety, FS

With the aim of studying the influence of cohesion, c on the factor of safety of the soil, different values of c changing from 30 to 15 kPa were chosen, while the unit weight of the soil and the friction angle were kept constant at 30 kN/m^3 and 30 degrees, respectively.

The factor of safety values calculated for varying cohesion values are given in Table 4.

Table 4. Effect of Cohesion on FS

Model No	Unit Weight (kN/m^3)	Internal Friction Angle (°)	Cohesion (kPa)	Factor of Safety
1	30	30	30	1.31
2	30	30	25	1.18
3	30	30	20	1.01
4	30	30	15	0.83

The data in Table 4 shows that factor of safety decreases by reducing the value of cohesion. As discussed earlier, since cohesion is one of the resisting forces, the

obtained result is in harmony with the theory. Figure 22 (a) shows the influence of cohesion on failure surface (While Figure 22(b) is a zoomed version of (a)).

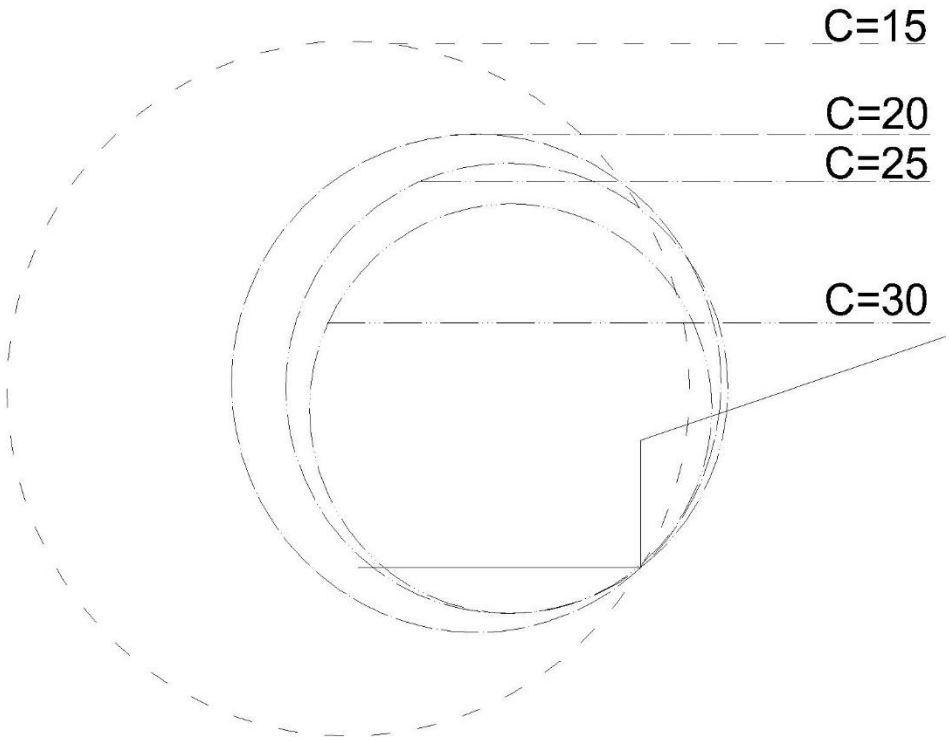

(a)

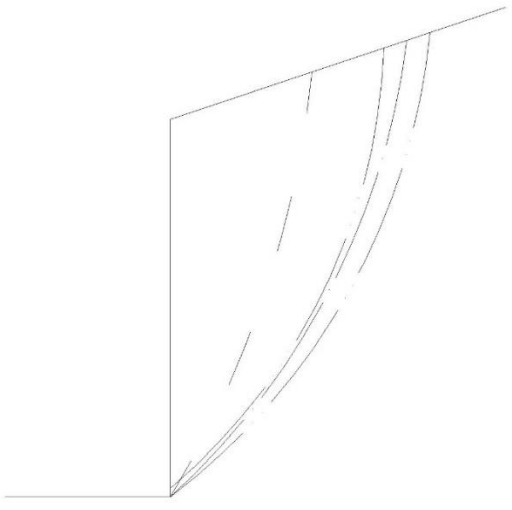

(b)

Figure 22. (a) Effect of C on Slip Surface, and (b) Exaggerated part of (a)

As it can be seen from the figure, except for c=20 kPa, other trials follow a logical order; by increasing the cohesion factor, failure surface (length of failure arc) decreases in order to achieve a same value for the cohesion force (which calculates by multiplying cohesion factor by length of failure arc). Besides that, smaller failure surface results in: a) a smaller value for the weight of the failure volume (smaller deriving force) and b) a smaller value for the friction force. On the other hand, with increasing the cohesion value, and hence decreasing the failure surface (length of failure arc), the factor of safety is increasing. This indicates that the reduction in deriving force is more dominant than the decrease in the friction effect.

4.2.3 Effect of Friction Angle, φ on the Factor of Safety, FS

To observe the influence of friction angle, cohesion is fixed to 30 kPa and the unit weight remains at 30 kN/m^3 while friction angle decreases from 30 to 15 degrees.

Table 5. Effect of φ on FS

Model No	Unit Weight (kN/m^3)	Internal Friction Angle (°)	Cohesion (kPa)	Factor of Safety
1	30	30	30	1.31
2	30	25	30	1.27
3	30	20	30	1.17
4	30	15	30	1.13

Table 5 shows that factor of safety decreases by dropping the value of internal friction angle; again this is normal since friction is the other resisting force.

Figure 23(a) shows the influence of friction angle on the failure surface (While Figure 23(b) is an exaggerated version of (a)).

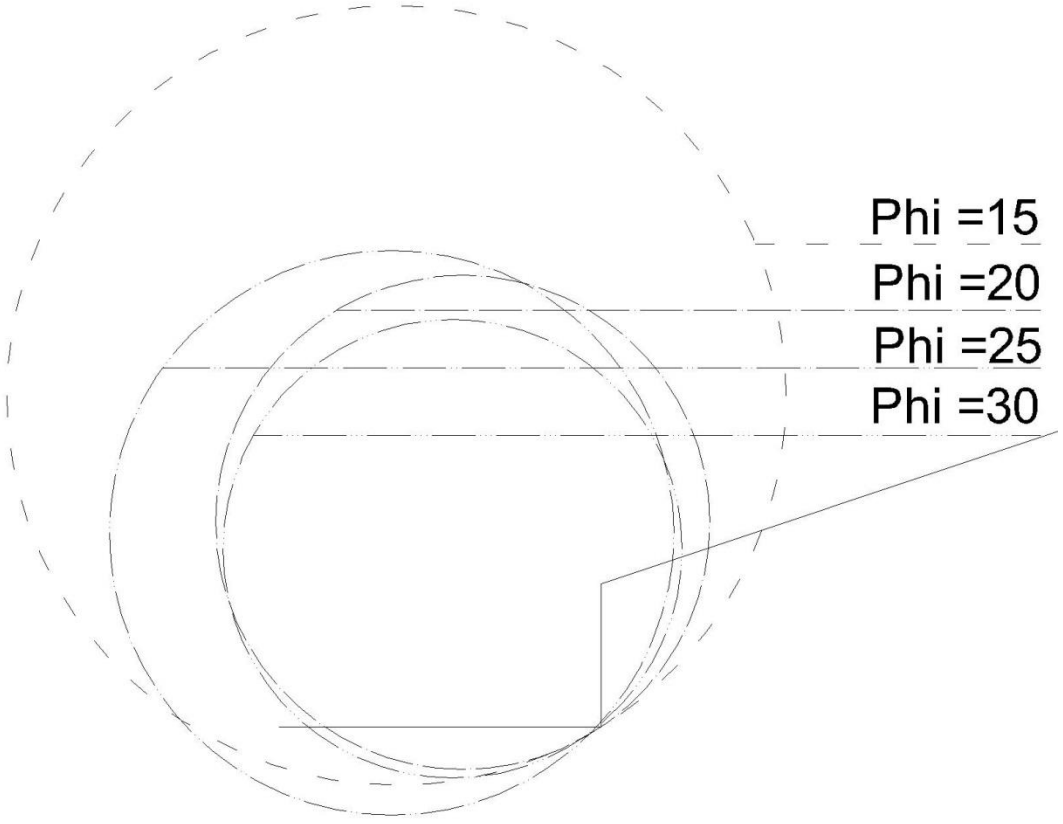

(a)

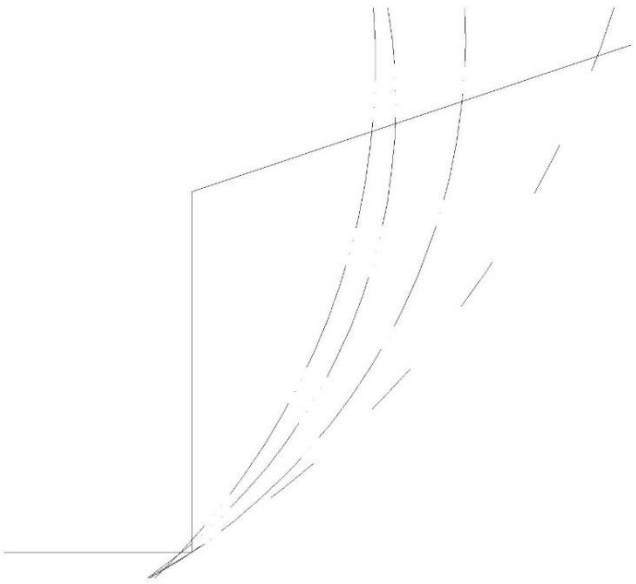

(b)

Figure 23. (a) Effect of φ on Slip Surface, and (b) Exaggerated Part of (a)

As it can be seen from the figure, same as the effect of cohesion, except for φ=30°, other trials follow a logical trend; by increasing the internal friction angle, failure surface (length of failure arc) decreases in order to achieve a same value for the friction force (which calculates by multiplying tangent of internal friction angle by length of failure arc). Besides that, smaller failure surface results in: a) a smaller value for the weight of the failure volume (smaller deriving force) and b) a smaller value for the cohesion force. In contrast, with increasing the internal friction angle, and hence decreasing the slip surface (length of failure arc), the factor of safety is decreasing. This indicates that the reduction in deriving force is less dominant than the decrease in the cohesion effect.

4.2.4 Effect of Slope Geometry on the Factor of Safety

With the intention of observing the effect of slope shape on the factor of safety, four different slope shapes have been analyzed with constant soil strength parameters: c = 15 kPa, γ = 15 kN/m^3, and φ = 15°.

Considering cases Number 1 and 2 together, and 3 and 4 together (Table 6), it is observed that increasing the angle of surface soil (Alpha – see Figure 24) will cause the slope to be less stable; this might be because of the fact that this amount of added soil to the top part will act like an overhead load increasing the deriving force and causing the factor of safety to decrease.

On the other hand, considering cases Number 1 and 3 together, and 2 and 4 together, it is observed that decreasing the slope angle (Beta), will cause the slope to be more stable; this might be because of the fact that by decreasing this angle, the length of

arc is increasing and this will lead to a more resisting force which will make the factor of safety increase.

Table 6. Effect of Slope Geometry on FS

Model No	Unit Weight (kN/m^3)	Internal Friction Angle (°)	Cohesion (kPa)	Factor of Safety
1	15	15	15	1.49
2	15	15	15	1.40
3	15	15	15	1.20
4	15	15	15	1.14

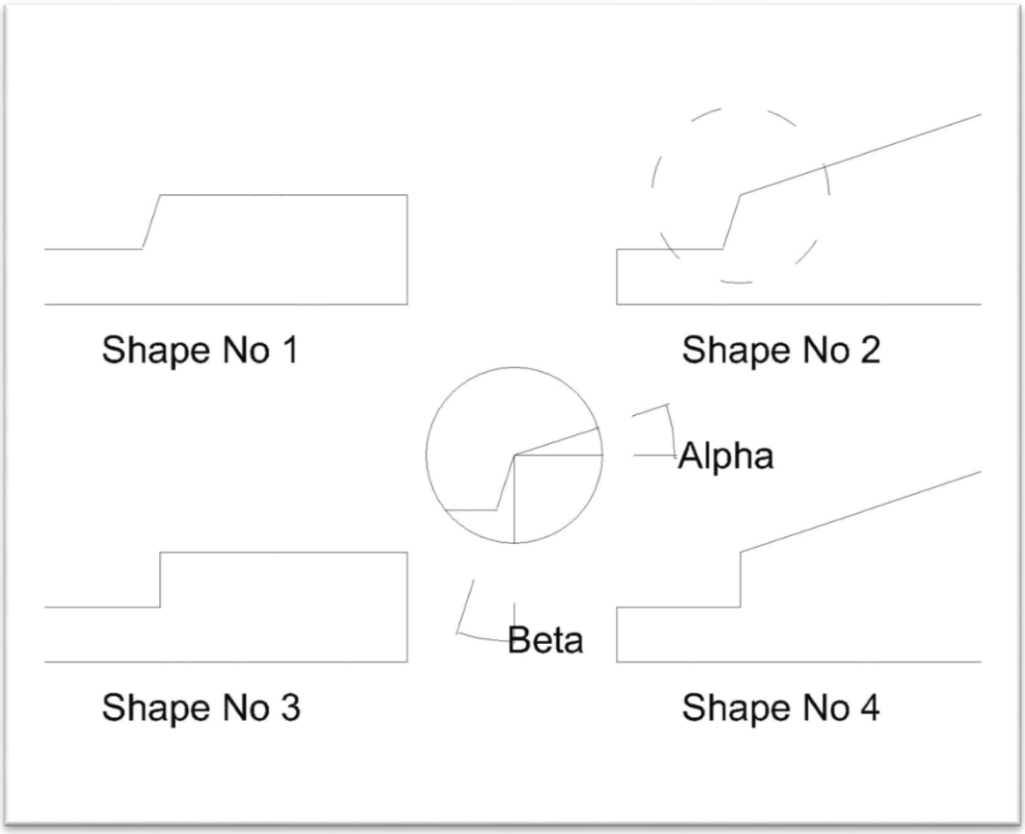

Figure 24. Effect of Slope Geometry on FS, Models

4.3 Effect of Soil Strength and Geometry Parameters on Slip Surface

Based on what have been discussed in previous section (4.2), it is predictable that there should be a correlation between soil strength parameters and slope geometry and the failure surface; in order to analyze this condition, the following models will be studied.

In this step, numerous models have been generated using GEO5 software. The output data in this part will be the factor of safety and coordinates of center of the slip circle and the radius of the circular failure surface. To find the length of failure slip and locating the entry point in the slope area, the circles were drawn by using AutoCAD software.

Figure 25 shows the general shape of the geometry of the slope that will be used in the first 72 of the models (before studying the slope geometry)

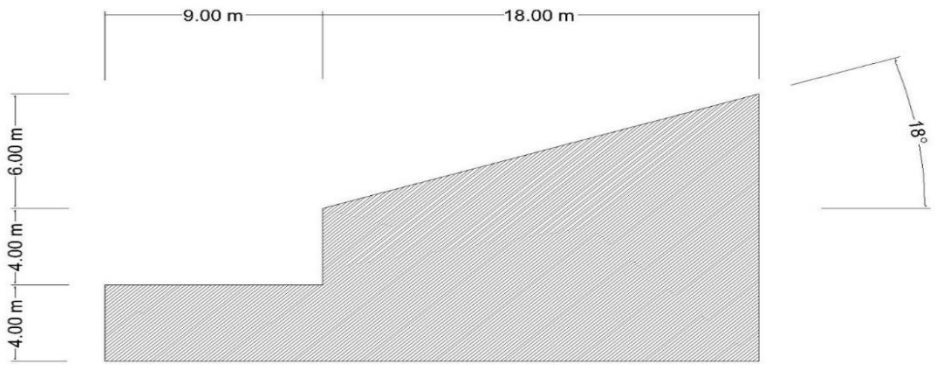

Figure 25. Slope Model Geometry

The generated models have been analyzed by considering different soil unit weight and shear strength parameters. The details of these parameters are given and discussed in the upcoming sections.

4.3.1 Effect of Cohesion, c on the Slip Surface

In this part, the soil's unit weight and friction angle remained constant at 15 kN/m^3 and 15° respectively, and the cohesion varied from 15 to 32 kPa.

Table 7. Models, Cohesion, c Values Selected for the Slip Surface Analyses

Model No	Unit Weight (kN/m^3)	Internal Friction Angle (°)	Cohesion (kPa)	λ	Entry Point Distance, l (m)	Length of Failure Arc (m)	Factor of Safety
1	15	15	15	0.75	2.92	5.90	1.08
2	15	15	16	0.80	2.97	5.93	1.14
3	15	15	17	0.85	3.05	5.99	1.21
4	15	15	18	0.90	3.13	6.10	1.26
5	15	15	19	0.96	3.27	6.03	1.33
6	15	15	20	1.01	3.23	6.16	1.39
7	15	15	21	1.06	3.29	6.17	1.45
8	15	15	22	1.11	3.24	6.17	1.50
9	15	15	23	1.16	3.26	6.18	1.56
10	15	15	24	1.21	3.33	6.27	1.63
11	15	15	25	1.26	3.38	6.31	1.69
12	15	15	26	1.31	3.47	6.37	1.75
13	15	15	27	1.36	3.40	6.34	1.81
14	15	15	28	1.41	3.44	6.32	1.87
15	15	15	29	1.46	3.56	6.44	1.93
16	15	15	30	1.51	3.74	6.56	2.00
17	15	15	31	1.56	3.52	6.44	2.06
18	15	15	32	1.61	3.57	6.51	2.11

4.3.2 Effect of Internal Friction Angle, φ on the Slip Surface

In this part, cohesion and unit weight remained constant at 15 kPa and 15 kN/m^3 respectively, while the friction angle varied from 16° to 32°.

Table 8. Models, Internal Friction Angles Chosen for the Slip Surface Analyses

Model No	Unit Weight (kN/m^3)	Internal Friction Angle (°)	Cohesion (kPa)	λ	Entry Point Distance, l (m)	Length of Failure Arc (m)	Factor of Safety
19	15	16	15	0.70	2.81	5.78	1.09
20	15	17	15	0.66	2.76	5.76	1.11
21	15	18	15	0.62	2.71	5.71	1.12
22	15	19	15	0.58	2.71	5.71	1.13
23	15	20	15	0.55	2.66	5.66	1.14
24	15	21	15	0.52	2.59	5.59	1.16
25	15	22	15	0.50	2.50	5.52	1.16
26	15	23	15	0.47	2.57	5.57	1.19
27	15	24	15	0.45	2.54	5.55	1.20
28	15	25	15	0.43	2.47	5.49	1.22
29	15	26	15	0.41	2.40	5.42	1.22
30	15	27	15	0.39	2.25	5.31	1.24
31	15	28	15	0.38	2.24	5.30	1.25
32	15	29	15	0.36	2.32	5.36	1.27
33	15	30	15	0.35	2.21	5.29	1.28
34	15	31	15	0.33	2.17	5.23	1.29
35	15	32	15	0.32	2.20	5.27	1.31

4.3.3 Effect of Unit Weight, φ on the Slip Surface

In this part, cohesion and friction angle remained constant at 15 kPa and 15°, while the unit weight varied from 16 to 31 kN/m^3.

Table 9. Models, Unit Weight Values Selected for the Slip Surface Analyses

Model No	Unit Weight (kN/m^3)	Internal Friction Angle (°)	Cohesion (kPa)	λ	Entry Point Distance, I (m)	Length of Failure Arc (m)	Factor of Safety
36	16	15	15	0.71	2.79	5.80	1.02
37	17	15	15	0.66	2.74	5.78	0.97
38	18	15	15	0.63	2.73	5.74	0.93
39	19	15	15	0.59	2.68	5.71	0.89
40	21	15	15	0.54	2.60	5.68	0.82
41	23	15	15	0.49	2.52	5.61	0.77
42	25	15	15	0.45	2.48	5.54	0.73
43	27	15	15	0.42	2.47	5.50	0.68
44	29	15	15	0.39	2.23	5.49	0.65
45	31	15	15	0.36	2.83	5.28	0.61

4.3.4 Effect of Cohesion, c, and Unit Weight, γ on the Slip Surface

In this part, the friction angle remained constant at 15° and for both cohesion and unit weight, the values were varied from 16 to 31 for both parameters.

Table 10. Models, Unit Weight and Cohesion Values Selected for the Slip Surface Analyses

Model No	Unit Weight (kN/m^3)	Internal Friction Angle (°)	Cohesion (kPa)	λ	Entry Point Distance, I (m)	Length of Failure Arc (m)	Factor of Safety
46	16	15	16	0.75	2.88	5.86	1.08
47	18	15	18	0.75	2.88	5.86	1.08
48	20	15	20	0.75	2.88	5.86	1.08
49	22	15	22	0.75	2.88	5.86	1.08
50	24	15	24	0.75	2.88	5.86	1.08
51	26	15	26	0.75	2.88	5.86	1.08
52	28	15	28	0.75	2.88	5.86	1.08
53	30	15	30	0.75	2.88	5.86	1.08
54	31	15	31	0.75	2.88	5.86	1.08

4.3.5 Effect of Internal Friction Angle, φ, and Unit Weight, φ on the Slip Surface

In this part, cohesion factor remained constant at 15 kPa while the other parameters varied from 15 to 31.

Table 11. Models, Unit Weight and Internal Friction Angle Values Selected for the Slip Surface Analyses

Model No	Unit Weight (kN/m^3)	Internal Friction Angle (°)	Cohesion (kPa)	λ	Entry Point Distance, I (m)	Length of Failure Arc (m)	Factor of Safety
55	16	16	15	0.66	2.84	5.81	1.04
56	18	18	15	0.52	2.61	5.61	0.97
57	20	20	15	0.41	2.51	5.54	0.92
58	22	22	15	0.34	2.32	5.36	0.88
59	24	24	15	0.28	2.08	5.17	0.85
60	26	26	15	0.24	1.94	5.07	0.83
61	28	28	15	0.20	1.66	4.85	0.81
62	30	30	15	0.17	1.65	4.84	0.80
63	31	31	15	0.16	1.57	4.79	0.79

4.3.6 Effect of Internal Friction Angle, φ, and Cohesion, c on the Slip Surface

In this section, cohesion and friction angle varied from 16 to 31 while unit weight remained constant at 15 kN/m^3.

Table 12. Models, Internal Friction Angle and Cohesion Values Selected for the Slip Surface Analyses

Model No	Unit Weight (kN/m^3)	Internal Friction Angle (°)	Cohesion (kPa)	λ	Entry Point Distance, l (m)	Length of Failure Arc (m)	Factor of Safety
64	15	16	16	0.75	2.58	5.57	1.16
65	15	18	18	0.75	2.84	5.81	1.30
66	15	20	20	0.74	3.01	5.96	1.45
67	15	22	22	0.73	3.01	5.97	1.60
68	15	24	24	0.72	3.02	5.94	1.76
69	15	26	26	0.72	3.08	6.03	1.90
70	15	28	28	0.71	3.01	5.96	2.05
71	15	30	30	0.70	3.03	5.97	2.20
72	15	31	31	0.69	2.94	5.91	2.28

4.3.7 Effect of Slope Geometry on the Slip Surface

It has been shown that slope geometry has a direct correlation with the slope stability as well as soil strength properties (Namdar, 2011).

In the last series of models, soil strength parameters remained constant at following values, while the angles α and β (shown in Figure 24) in slope geometry varied from 0° to 18°.

Internal friction angle = 15°, Cohesion = 15 kPa, Unit weight = 15 kN/m^3

Table 13. Effect of Slope Geometry on the Slip Surface

Model No	α (°)	β (°)	----------Failure Surface----------				Factor of Safety
			Center		Radius (m)	Length of arc (m)	
			X (m)	Y (m)			
1	18	0	4.81	21.27	7.51	6.16	1.11
2	17	0	3.33	23.96	10.57	6.94	1.14
3	16	0	3.45	23.79	10.37	6.81	1.15
4	15	0	3.14	24.13	10.82	6.75	1.15
5	14	0	3.12	23.89	10.63	6.53	1.16
6	13	0	2.76	24.24	11.14	6.51	1.16
7	12	0	3.29	23.55	10.25	6.27	1.16
8	11	0	2.95	23.92	10.75	6.22	1.17
9	10	0	2.54	24.34	11.32	6.16	1.18
10	9	0	3.08	23.58	10.40	5.96	1.17
11	8	0	5.08	20.61	6.70	5.12	1.18
12	7	0	5.77	20.45	6.21	5.28	1.19
13	6	0	5.12	21.75	7.75	5.72	1.19
14	5	0	2.29	24.11	11.28	5.60	1.19
15	4	0	2.53	24.00	11.05	5.56	1.19
16	3	0	1.99	24.54	11.81	5.50	1.20
17	2	0	1.75	24.31	11.77	5.31	1.19
18	1	0	1.99	24.20	11.54	5.26	1.20
19	0	0	1.37	24.81	12.40	5.21	1.20
20	0	1	2.73	23.36	10.35	5.11	1.22
21	0	2	2.95	23.36	10.14	5.13	1.25
22	0	3	4.01	22.53	8.84	5.21	1.27
23	0	4	4.04	22.54	8.82	5.28	1.28
24	0	5	4.54	21.75	7.86	5.24	1.28
25	0	6	4.16	22.11	8.34	5.30	1.29
26	0	7	4.28	22.11	8.23	5.34	1.32
27	0	8	5.44	19.94	5.71	4.89	1.33
28	0	9	5.67	20.75	6.27	5.32	1.36
29	0	10	5.43	20.98	6.57	5.37	1.37
30	0	11	5.45	20.99	6.55	5.45	1.39
31	0	12	5.19	21.24	6.88	5.51	1.40
32	0	13	5.24	20.95	6.55	5.41	1.42
33	0	14	6.15	20.22	5.47	5.50	1.45
34	0	15	6.28	20.10	5.32	5.70	1.46
35	0	16	6.28	20.10	5.33	5.70	1.47
36	0	17	5.79	20.59	5.92	5.71	1.48
37	0	18	5.78	20.37	5.67	5.59	1.50

4.4 Effect of Soil Strength and Geometry Parameters on Factor of Safety

In order to weigh the effect of soil strength parameters and geometry parameters on the factor of safety, the factor of safety versus these soil strength parameters were drawn and offered in the subsequent figures.

4.4.1 Effect of Cohesion, c on the Factor of Safety, FS

In this part, the influence of cohesion on the factor of safety has been shown. As it was expected, increasing the cohesion value which is a resistant force increased the value of factor of safety. The linear relation between cohesion and factor of safety can be seen in Figure 26.

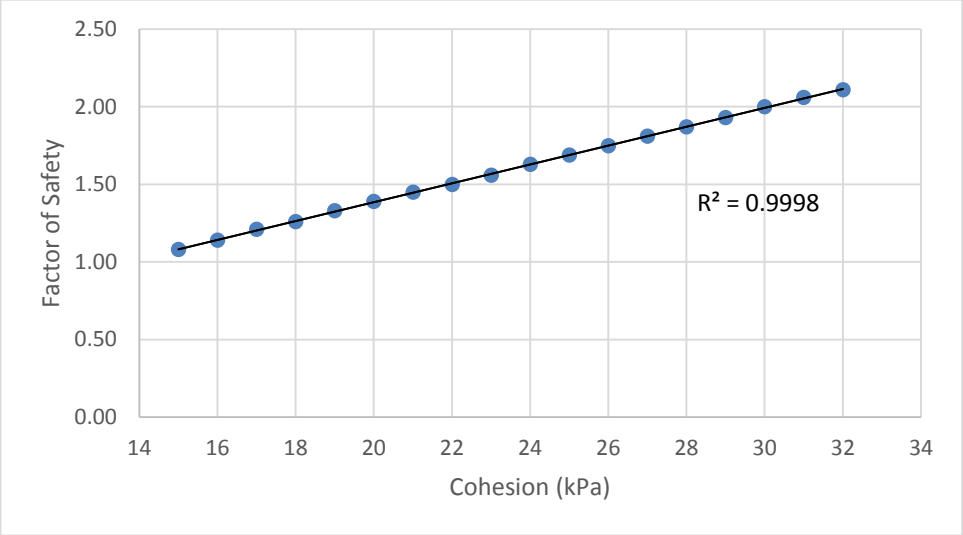

Figure 26. Effect of Cohesion, c on the Factor of Safety, FS

4.4.2 Effect of Internal Friction Angle on the Factor of Safety

In this part, the influence of friction angle on the factor of safety has been shown. As it was expected, increasing the friction angle which is the other resistant force increased the value of factor of safety. As it can be seen from Figure 27, the relationship between the friction angle, ϕ and the factor of safety, FS is almost linear with a squared R factor of 0.99.

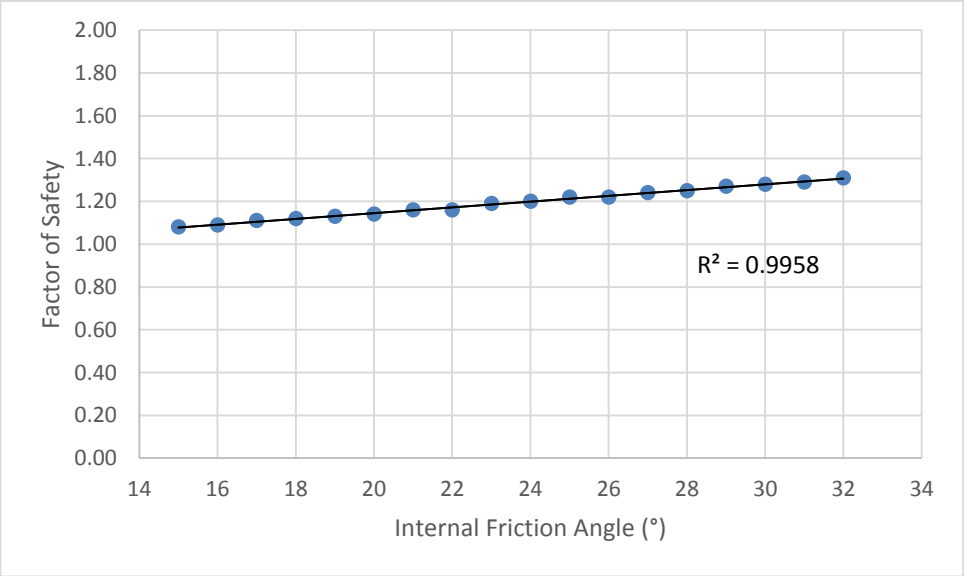

Figure 27. Effect of Friction Angle on the Factor of Safety

4.4.3 Effect of Unit Weight on the Factor of Safety

The effect of unit weight of the soil on the factor of safety was shown in Figure 28. As it can be seen from the figure, the unit weight as the main driving force applied in the soil mass is inversely proportional to the factor of safety.

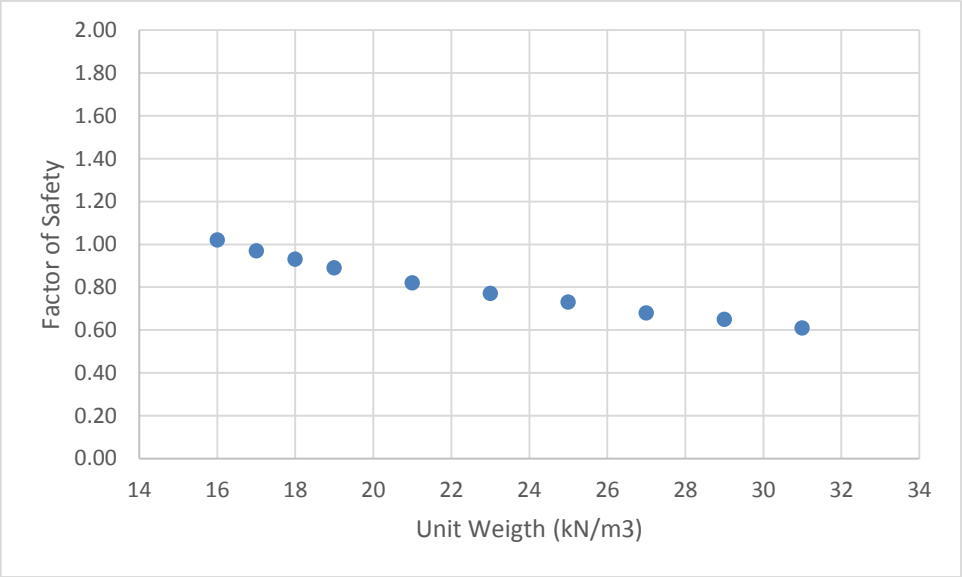

Figure 28. Effect of Unit Weight on the Factor of Safety

4.4.4 The Combined Effect of Cohesion and the Unit Weight on the Factor of Safety

The effect of cohesion together with the unit weight of the soil on the factor of safety was studied in this section. Here, cohesion and the unit weight of the soil were increased together, while their ratio remained constant. The results specify that the potential slip surface is touched by the combination of c and φ whose function is defined as λ which is equal to:

$$\lambda = c/(\gamma\ h\ \ tan\,\varphi\ ) \qquad \text{Equation 28}$$

Figure 29 indicates that factor of safety remains constant while λ value remains the same.

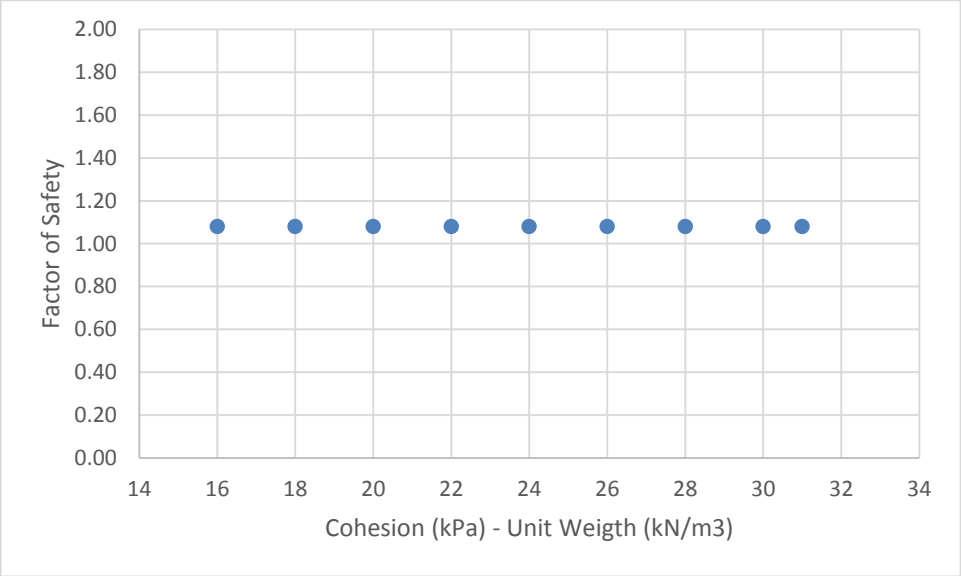

Figure 29. The Combined Effect of Cohesion and the Unit Weight on the Factor of Safety

4.4.5 The Combined Effect of Internal Friction and the Unit Weight on the Factor of Safety

In this part, the value of internal friction angle by unit weight is increasing by increasing both of them. Hence, the factor of safety versus tan (φ) * **γ** curve was drawn and shown in Figure 30.

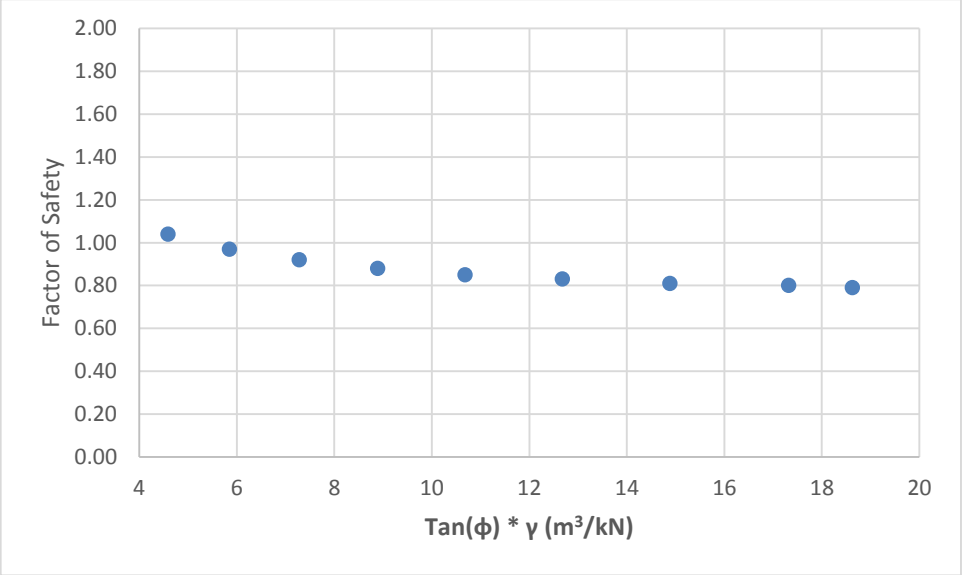

Figure 30. The Combined Effect of Internal Friction Angle and the Unit Weight on the Factor of Safety

As it can be seen in Figure 30, reduction in the factor of safety value was obtained by increasing the value of tan (φ) * **γ.** This is because of the movement of failure surface to the top, and hence decreasing the length of failure arc and so a decrease in effect of resisting forces.

4.4.6 The Combined Effect of Internal Friction and Cohesion on the Factor of Safety

In this part, since the potential failure surface is anticipated to be affected by the combination of c and φ values, the relation between the factor of safety and $c\ and\ tan\ (\varphi)$ is shown in Figure 31. Since both of these shear strength parameters are resisting forces, increasing these two values leads to an increase in the value of factor of safety.

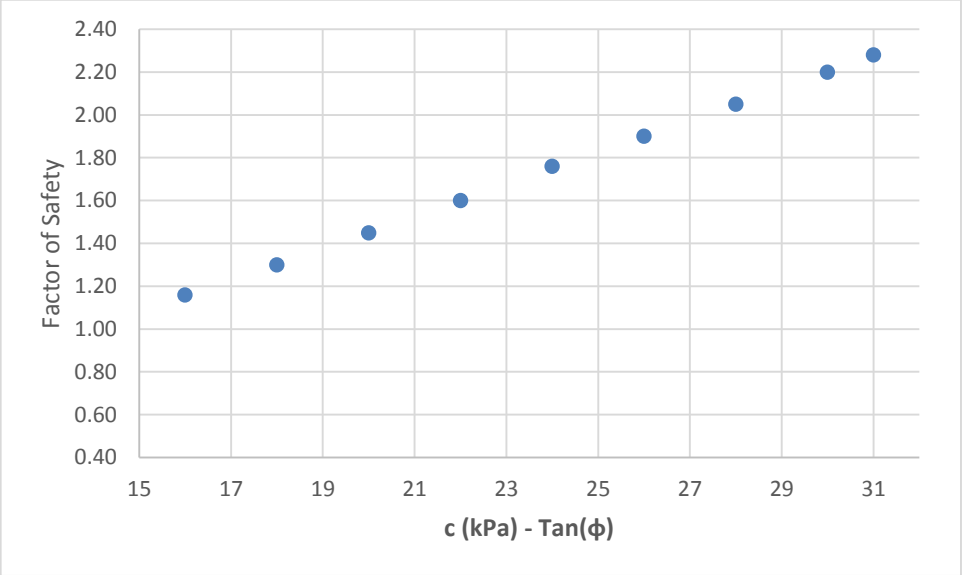

Figure 31. The Combined Effect of Internal Friction Angle and Cohesion on the Factor of Safety

4.4.7 Effect of Slope Geometry on the Factor of Safety

To study the effect of geometry on the factor of safety, two slope angles α, and β (introduced in the methodology section) have been varied and their effect on factor of safety has been observed. The results are presented in the following figures.

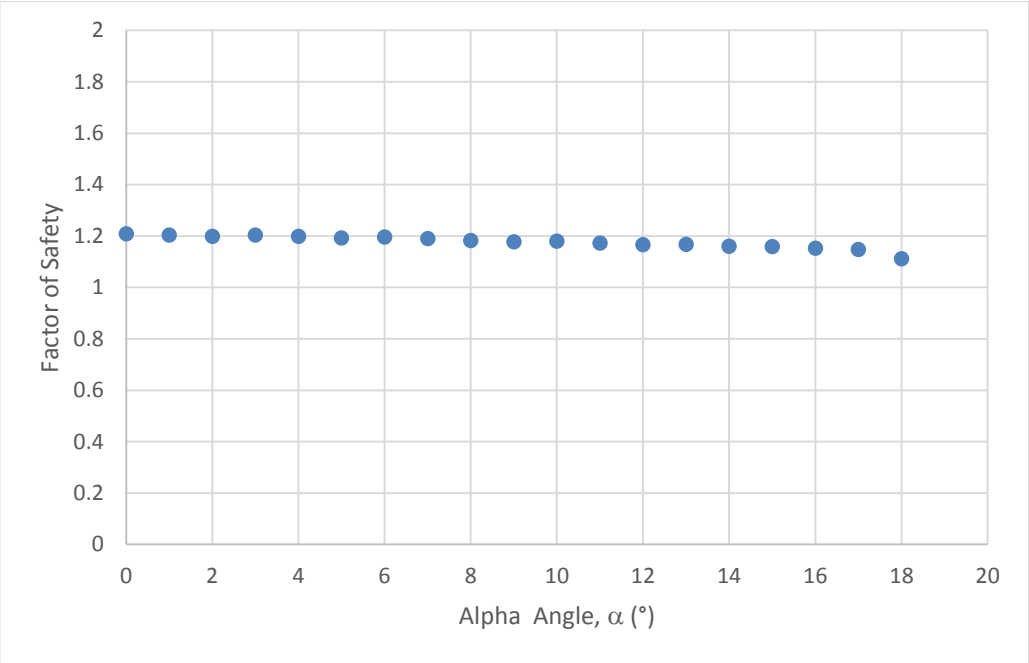

Figure 32. Effect of Alpha Angle on Safety Factor

Figure 32 shows that by changing the alpha angle, no noteworthy variation is observed in the factor of safety until 16°, and afterwards FS starts to decrease. This is because of the fact that increasing alpha angle can be acted as if adding an extra overhead surcharge on the slope surface. Until the angle of 16°, increasing the failure surface and consequently increasing the length of arc, generate more resisting force and make the factor of safety constant. Although this increase in the failure surface generates more resisting force, it generates an increase in deriving force (weight of failure surface) simultaneously. Therefore, the factor of safety stays constant. For angles greater than 16°, the increase in deriving force approaches to the resisting force value and from this value of angle onwards, the deriving force gets bigger than resisting force, and thus, a drop can be seen in the factor of safety value.

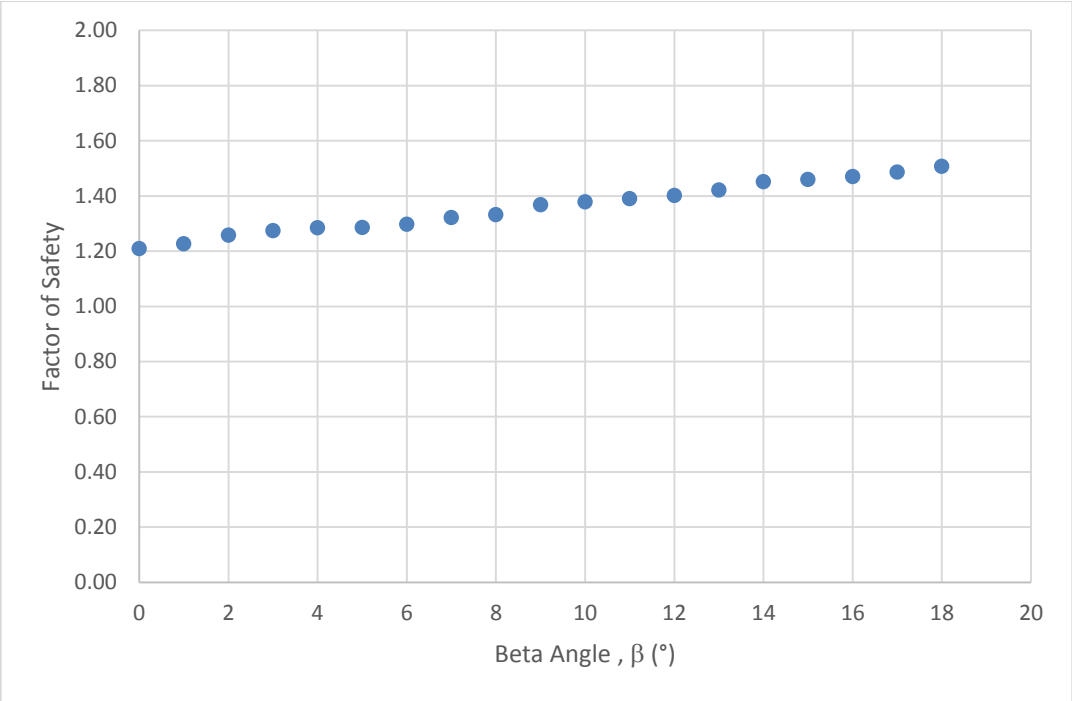

Figure 33. Effect of Beta, β Angle on Factor of Safety

Figure 33 shows that by increasing the Beta angle, the factor of safety increases significantly. The reason for this behavior is that by increasing the beta angle, only the length of failure arc increases (as resisting force) and the mass of failure shape (as deriving force) remains almost constant. So, increase in the length of the arc increases the resisting force and hence the factor of safety increases.

4.5 Effect of Soil Strength and Geometry Parameters on Slip Surface

En route for study the effect of each soil parameter on slip surface, length of failure arc, as a quantitative variable has been chosen to be studied. The following figures will be presented in order to show this effect.

4.5.1 Effect of Cohesion, c on the Length of Failure Arc, L

In Figure 34, the influence of cohesion on length of failure surface is shown.

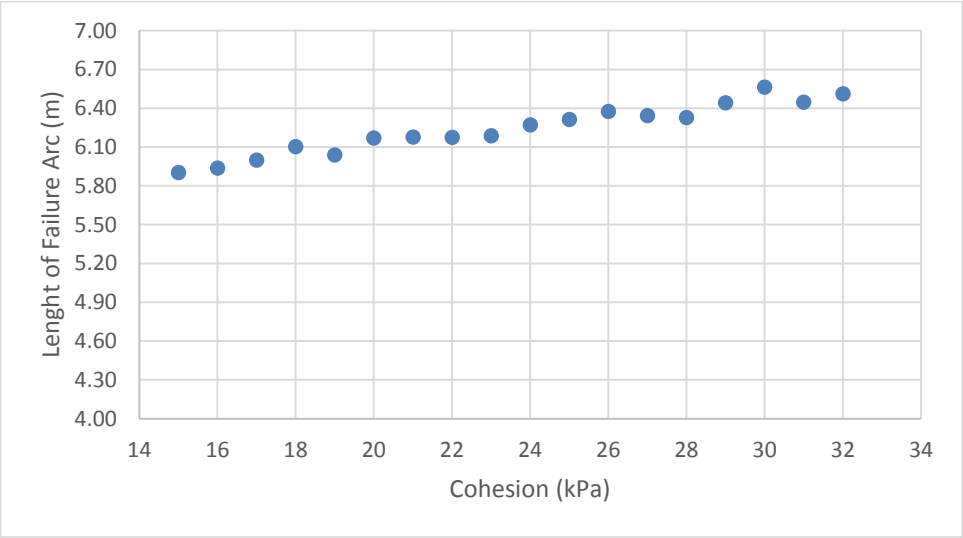

Figure 34. Effect of Cohesion, c on the Length of Failure Arc, L

It can be seen in the figure that with increasing the value of cohesion, length of failure surface will increase. The reason is that, in the case of the location of the failure surface remaining constant, as the c factor increases, the resisting force gets bigger as well as factor of safety. So to find the minimum FS (which is the main goal of the slope stability analysis), the driving force should increase, which can be achieved by increasing the slope failure area. This leads to a greater length of failure arc (L) and thus smaller factor of safety value.

4.5.2 Effect of Internal Friction Angle, φ on the Length of Failure Arc, L

Figure 35 represents the effect of internal friction on the length of failure arc.

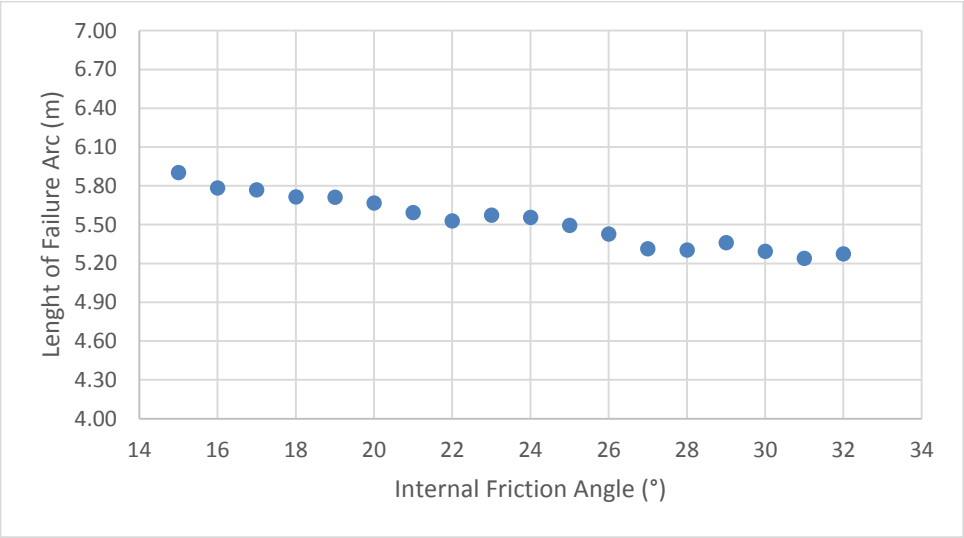

Figure 35. Effect of Internal Friction, γ on the Length of Failure Arc, L

Referring to the same explanation in the previous section, it can be expected that length of arc, L should be in a direct relation with phi, but as it can be seen in Figure 35, L and phi are inversely related.

This inverse relation is in line with (Jiang & Yamagami, 2006) study which states that "when the slope geometry, unit weight and pore water pressure distribution in a homogeneous soil slope are given, the location of the critical slip surface for a particular method of slices is related only to $\frac{c}{Tan\,(\varphi)}$ ratio of that slope", this study shows that the position of the slip surface and thus the length of failure arc is in an inverse relation with internal friction angle.

4.5.3 Effect of Unit Weight, γ on the Length of Failure Arc, L

In this section, effect of unit weight on the length of arc is studied.

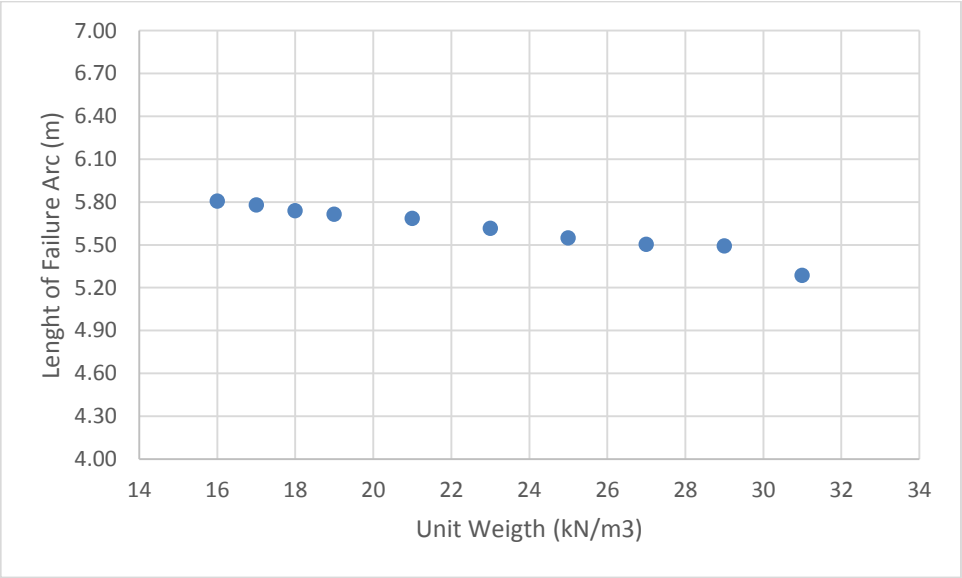

Figure 36. Effect of Unit Weight on the Length of Failure Arc, L

As it can be seen in Figure 36 by increasing the unit weight, weight of the falling shape increases, and this leads to a smaller factor of safety. In other words, by considering λ, the failure slip surface moves toward the face of the slope, meanwhile by decreasing L, the effects of cohesion and friction angle as resistance forces decrease, and hence smaller factor of safety will be achieved.

4.5.4 The Combined Effect of Cohesion and Unit Weight on the Length of Failure Arc, L

In this part, cohesion and unit weight decrease together in a way that their ratio remains constant. The result can be seen in Figure 37.

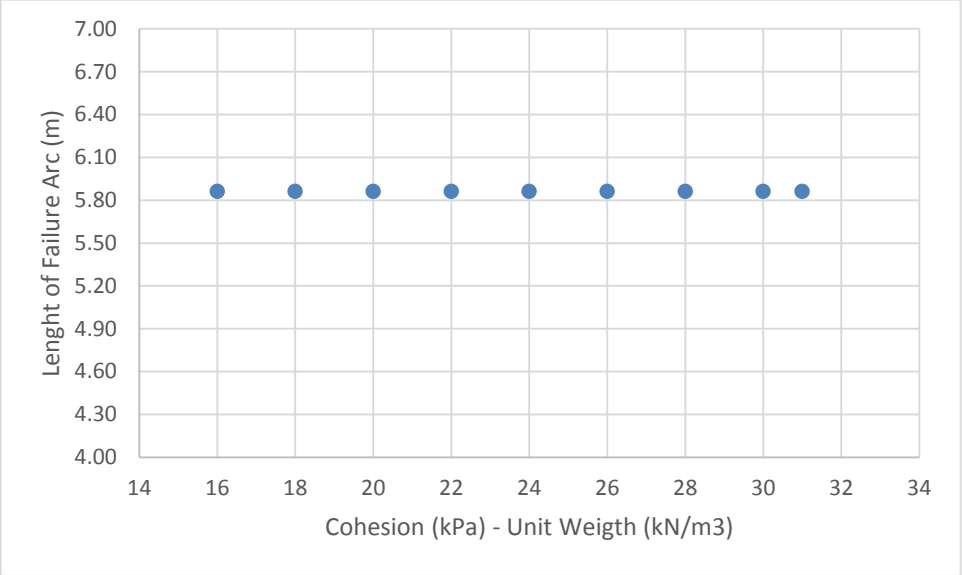

Figure 37. The Combined Effect of Cohesion and Unit Weight on the Length of Failure Arc, L

Constant ratio of unit weight over c , leads to a constant λ. As it has been mentioned in study of (Lin & Cao, 2011), this means same failure shape and hence a constant value for L.

4.5.5 The Combined Effect of Internal Friction Angle and the Unit Weight on the Length of Failure Arc, L

In order to show the influence of variation of unit weight and internal friction angle on length of failure arc, the Figure 38 has been drawn.

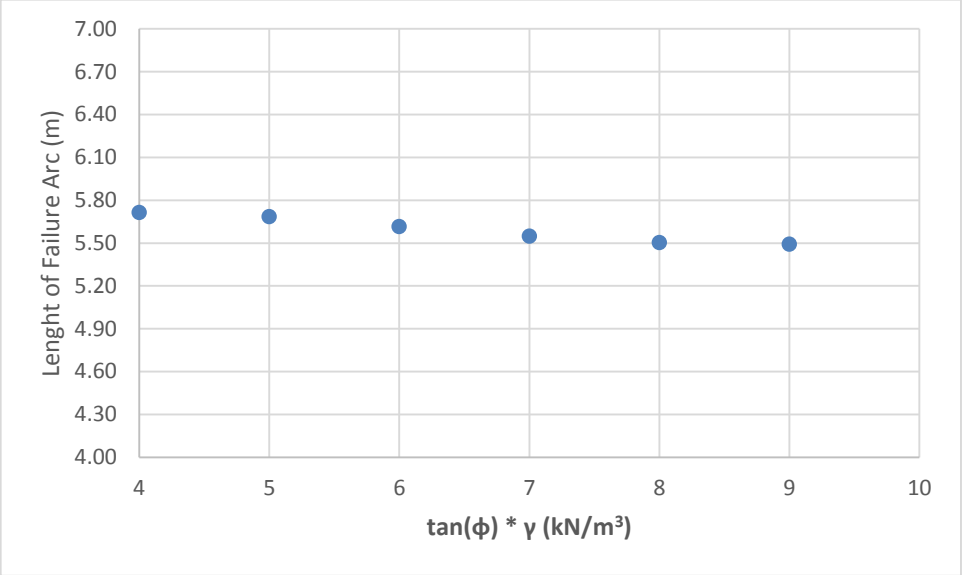

Figure 38. The Combined Effect of Internal Friction Angle and the Unit Weight on the Length of Failure Arc, L

It can be seen that increasing the value of $\gamma * Tan\,\varphi$ will lead to a decrease in the length of failure surface. This is in harmony when considering the value of λ, by increasing this value, λ decreases; smaller λ means a failure surface closer to the slope surface and hence smaller length of failure arc.

4.5.6 The Combined Effect of Internal Friction Angle and Cohesion on the Length of Failure Arc, L

To illustrate the combined effect of varying cohesion and internal friction angle on the length of failure arc, the following figure (Figure 39) has been drawn.

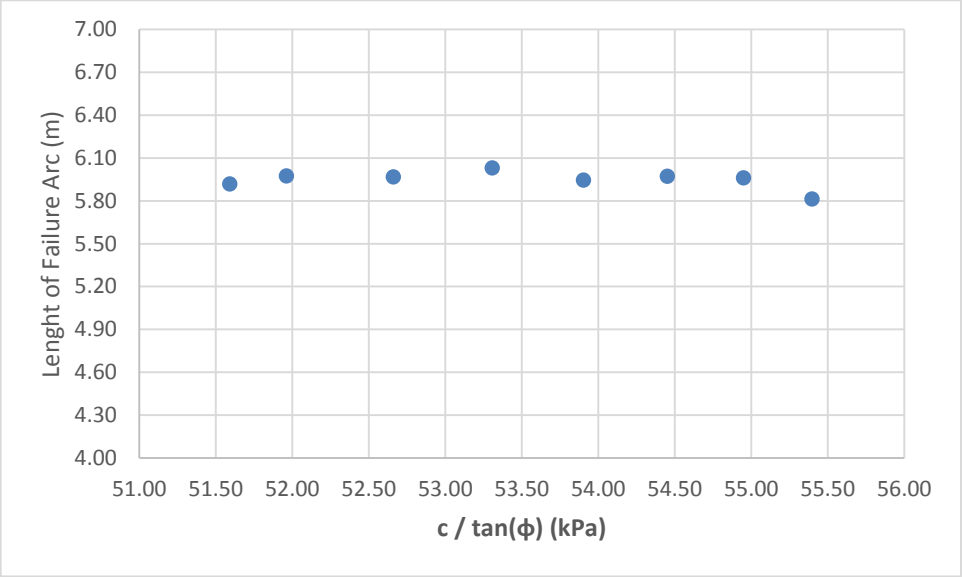

Figure 39. The Combined Effect of Internal Friction Angle and Cohesion on the Length of Failure Arc, L

From Figure 39, it can be seen that at relatively constant value of $c/tan\,\varphi$ (51.50~55.50 kPa), L will remain relatively constant. Since constant $c/tan\,\varphi$ leads to a constant λ, and constant λ means a constant failure surface, the length of arc remains constant as well.

4.5.7 Effect of Slope Geometry on the Length of Failure Arc, L

To observe the effect of slope geometry on the failure surface, length of failure arc as a quantitative value has been measured and drawn in the following figures (Figure 44 and Figure 45).

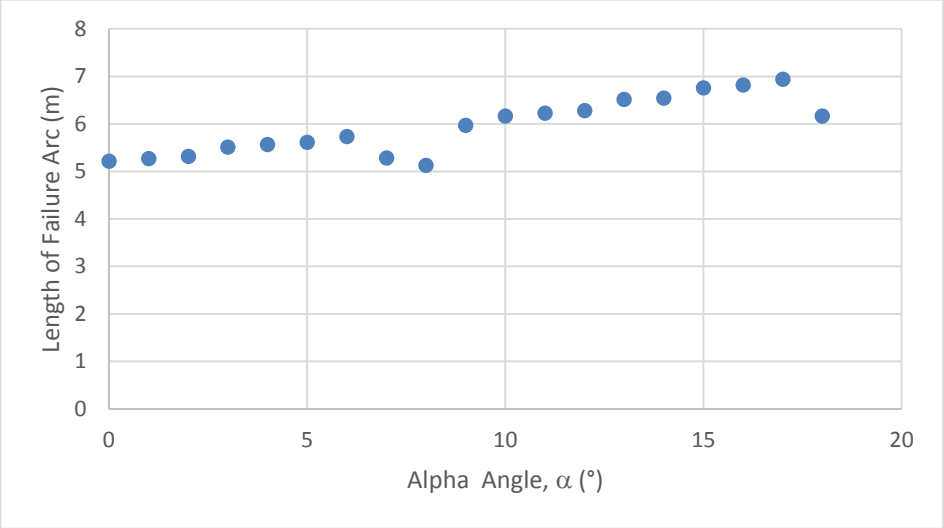

Figure 40. Effect of Alpha Angle on Length of Failure Arc

Results of analyzing the models, show that, by increasing the Alpha angle, the position of the failure surface does not vary significantly. The reason for increase in the length of failure arc is just the movement of the slope surface and hence the extension of the failure arc, [Figure 41 (a) and (b)].

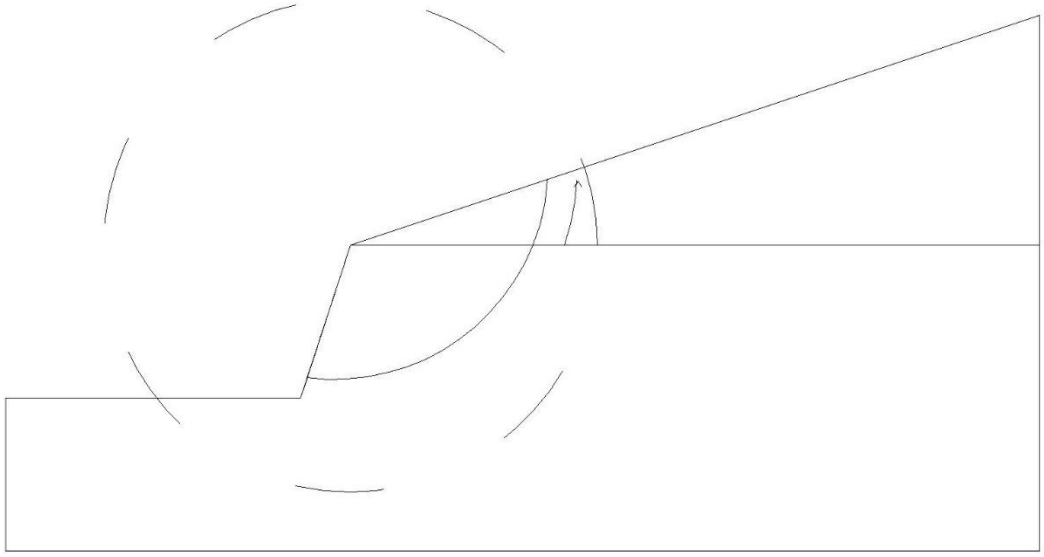

(a)

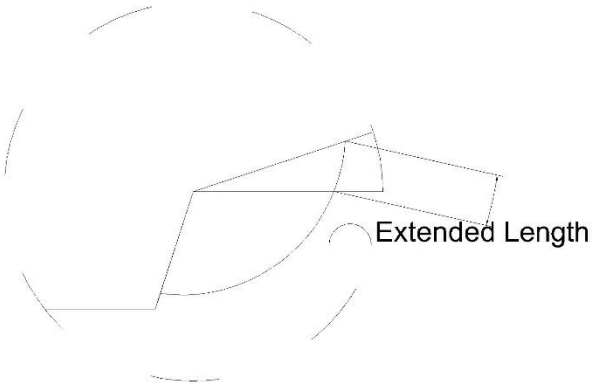

(b)

Figure 41. (a) Effect of Alpha on length of Arc and (b) Exaggerated Part of (a)

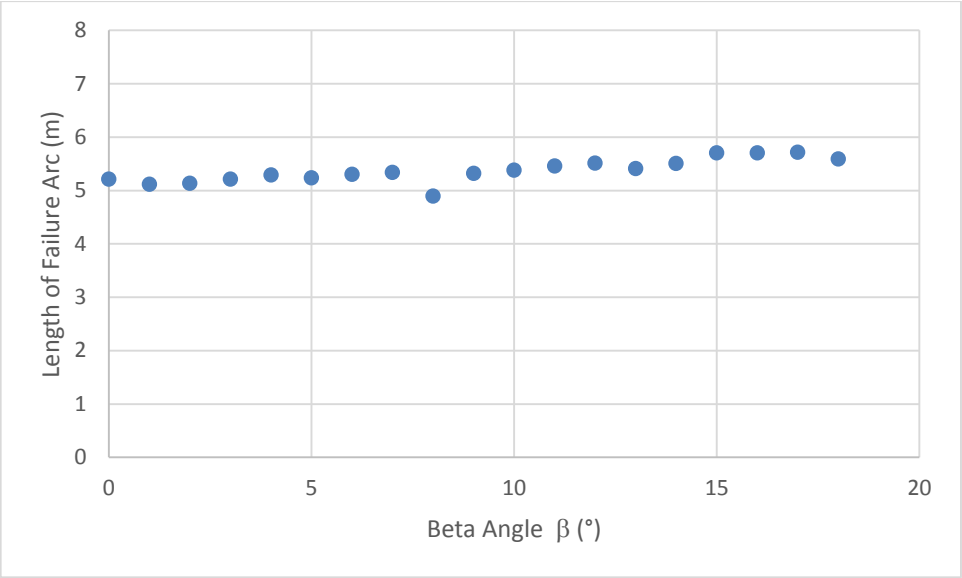

Figure 42. Effect of Beta Angle on Length of Failure Arc

By increasing the value of beta angle, (the other parameters in Equation 28 not changing, and thus not affecting the value of λ) the depth of the failure surface would not change. On the other hand, increase in the beta angle will move the slope surface to the left and this will make the failure arc to be extended as can be seen in Figure 43 (b).This will lead to a slightly larger length of failure arc.

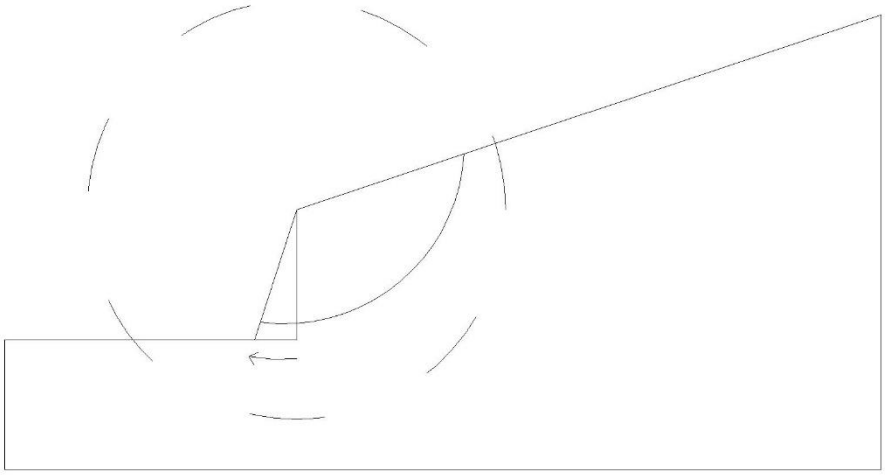

(a)

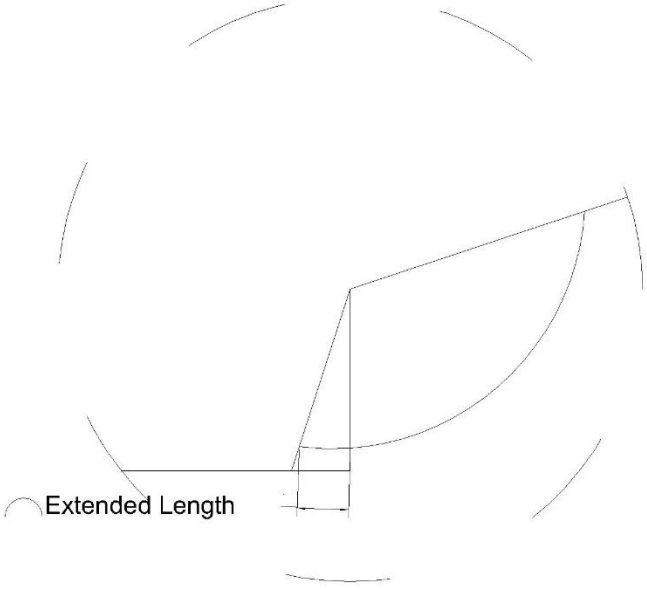

(b)

Figure 43. (a) Effect of Beta on Length of Arc and (b) Exaggerated part of (a)

4.6 Re-Analyzing Models by SLOPE/W and Comparison of Results

In order to validate the results of the GEO5 program, obtained in section 4.3, the studied models have been re-analyzed using SLOPE/W software program. Results of these analyzes can be found in Table 14 throw 19.

Table 14. Models, Cohesion, c Values Selected for the Slip Surface Analyses – [SLOPE/W]

Model No	Unit Weight (kN/m^3)	Internal Friction Angle (°)	Cohesion (kPa)	----------Failure Surface----------				Factor of Safety
				Center		Radius (m)	Length of Arc (m)	
				X (m)	Y (m)			
1	15	15	15	5.86	21.18	6.93	6.69	1.12
2	15	15	16	3.72	23.80	10.26	7.19	1.19
3	15	15	17	3.45	24.39	10.90	7.39	1.25
4	15	15	18	3.45	24.39	10.90	7.39	1.31
5	15	15	19	3.96	23.97	10.28	7.41	1.37
6	15	15	20	3.68	24.56	10.94	7.61	1.44
7	15	15	21	3.68	24.56	10.94	7.61	1.49
8	15	15	22	4.82	21.92	8.08	6.62	1.52
9	15	15	23	6.11	21.87	7.45	7.34	1.61
10	15	15	24	3.89	24.74	11.00	7.84	1.67
11	15	15	25	4.50	22.14	8.44	6.60	1.70
12	15	15	26	3.84	22.25	8.90	6.37	1.77
13	15	15	27	2.70	25.81	12.51	7.80	1.85
14	15	15	28	4.09	24.92	11.06	8.07	1.91
15	15	15	29	4.09	24.92	11.06	8.07	1.97
16	15	15	30	4.09	24.92	11.06	8.07	2.03
17	15	15	31	4.09	24.92	11.06	8.07	2.09
18	15	15	32	3.54	25.43	11.77	8.04	2.15

Table 15. Models, Internal Friction Angles Chosen for the Slip Surface Analyses – [SLOPE/W]

Model No	Unit Weight (kN/m^3)	Internal Friction Angle (°)	Cohesion (kPa)	----------Failure Surface----------				Factor of Safety
				Center		Radius (m)	Length of Arc (m)	
				X (m)	Y (m)			
19-0	15	15	15	5.86	21.18	6.93	6.69	1.12
19	15	16	15	4.44	21.18	7.68	6.00	1.11
20	15	17	15	4.90	21.03	7.19	6.12	1.15
21	15	18	15	2.94	24.04	10.88	6.95	1.18
22	15	19	15	3.18	23.47	10.28	6.75	1.19
23	15	20	15	2.65	23.86	10.90	6.74	1.21
24	15	21	15	5.03	20.64	6.80	5.94	1.20
25	15	22	15	2.87	23.31	10.32	6.54	1.23
26	15	23	15	4.10	20.54	7.26	5.28	1.24
27	15	24	15	4.20	22.01	8.49	6.39	1.26
28	15	25	15	2.52	23.15	10.40	6.45	1.28
29	15	26	15	2.38	20.36	8.51	5.05	1.27
30	15	27	15	4.78	20.19	6.56	5.31	1.29
31	15	28	15	4.60	20.10	6.73	5.46	1.26
32	15	29	15	5.62	20.00	5.94	5.59	1.32
33	15	30	15	4.95	20.87	7.12	6.03	1.35
34	15	31	15	4.15	21.35	7.99	5.99	1.36
35	15	32	15	2.40	19.93	8.23	4.90	1.34

Table 16. Models, Unit Weight Values Selected for the Slip Surface Analyses – [SLOPE/W]

Model No	Unit Weight (kN/m^3)	Internal Friction Angle (°)	Cohesion (kPa)	----------Failure Surface----------				Factor of Safety
				Center		Radius (m)	Length of Arc (m)	
				X (m)	Y (m)			
36-0	15	15	15	5.86	21.18	6.93	6.69	1.12
36	16	15	15	3.46	23.64	10.26	6.97	1.07
37	17	15	15	3.46	23.64	10.26	6.97	1.02
38	18	15	15	2.94	24.04	10.88	6.95	0.98
39	19	15	15	3.18	23.47	10.28	6.75	0.93
40	21	15	15	2.65	23.86	10.90	6.74	0.87
41	23	15	15	5.59	26.48	6.45	6.08	0.79
42	25	15	15	3.92	20.43	7.43	5.43	0.73
43	27	15	15	3.36	20.33	7.76	5.24	0.69
44	29	15	15	2.67	20.24	8.21	5.06	0.66
45	31	15	15	5.41	14.99	6.15	5.69	0.62

Table 17. Models, Unit Weight and Cohesion Values Selected for the Slip Surface Analyses – [SLOPE/W]

Model No	Unit Weight (kN/m^3)	Internal Friction Angle (°)	Cohesion (kPa)	----------Failure Surface----------				Factor of Safety
				Center		Radius (m)	Length of Arc (m)	
				X (m)	Y (m)			
46-0	15	15	15	5.86	21.18	6.93	6.69	1.12
46	16	15	16	5.86	21.18	6.93	6.69	1.12
47	18	15	18	5.86	21.18	6.93	6.69	1.12
48	20	15	20	5.86	21.18	6.93	6.69	1.12
49	22	15	22	5.86	21.18	6.93	6.69	1.12
50	24	15	24	5.86	21.18	6.93	6.69	1.12
51	26	15	26	5.86	21.18	6.93	6.69	1.12
52	28	15	28	5.86	21.18	6.93	6.69	1.12
53	30	15	30	5.86	21.18	6.93	6.69	1.12
54	31	15	31	5.86	21.18	6.93	6.69	1.12

Table 18. Models, Unit Weight and Internal Friction Angle Values Selected for the Slip Surface Analyses – [SLOPE/W]

Model No	Unit Weight (kN/m³)	Internal Friction Angle (°)	Cohesion (kPa)	----------Failure Surface----------				Factor of Safety
				Center		Radius (m)	Length of Arc (m)	
				X (m)	Y (m)			
55-0	15	15	15	5.86	21.18	6.93	6.69	1.12
55	16	16	15	4.90	21.03	7.19	5.92	1.08
56	18	18	15	4.15	20.66	7.45	5.62	0.98
57	20	20	15	2.52	23.15	10.40	6.33	0.97
58	22	22	15	5.24	19.91	6.08	5.37	0.91
59	24	24	15	1.20	22.22	10.62	5.55	0.89
60	26	26	15	1.73	21.06	9.46	5.21	0.85
61	28	28	15	3.66	20.56	7.70	5.42	0.85
62	30	30	15	3.85	20.11	7.25	5.26	0.83
63	31	31	15	2.78	20.59	8.35	5.23	0.83

Table 19. Models, Internal Friction Angle and Cohesion Values Selected for the Slip Surface Analyses – [SLOPE/W]

Model No	Unit Weight (kN/m³)	Internal Friction Angle (°)	Cohesion (kPa)	----------Failure Surface----------				Factor of Safety
				Center		Radius (m)	Length of Arc (m)	
				X (m)	Y (m)			
64-0	15	15	15	5.86	21.18	6.93	6.69	1.12
64	15	16	16	5.86	26.18	6.93	6.69	1.19
65	15	18	18	3.21	24.21	10.88	7.17	1.36
66	15	20	20	3.21	24.21	10.88	7.17	1.52
67	15	22	22	3.21	24.21	10.88	7.17	1.67
68	15	24	24	4.01	21.25	7.89	5.67	1.83
69	15	26	26	2.94	21.30	8.73	5.58	1.96
70	15	28	28	3.75	21.24	8.15	5.79	2.09
71	15	30	30	3.21	24.21	10.88	7.17	2.31
72	15	31	31	3.46	23.64	10.26	6.97	2.37

The difference between the FSs obtained from both programs (GEO5 and SLOPE/W) are tabulated in Table 20, and these results will be compared using following formula.

$$\text{Difference} = \frac{\text{FS}_{\text{SLOPE/W}} - \text{FS}_{\text{Geo-5}}}{\text{FS}_{\text{Geo-5}}} * 100 \qquad \text{Equation 29}$$

Table 20. Differences in FSs between SLOPE/W and Geo 5

Model No	Factor of Safety		Difference (%)
	SLOPE/W	Geo 5	
1	1.12	1.08	3.66
2	1.19	1.14	4.52
3	1.26	1.21	3.89
4	1.32	1.26	4.33
5	1.38	1.33	3.27
6	1.44	1.39	3.47
7	1.50	1.45	3.20
8	1.53	1.50	1.83
9	1.61	1.56	3.17
10	1.68	1.63	2.92
11	1.71	1.69	1.05
12	1.78	1.75	1.46
13	1.86	1.81	2.53
14	1.92	1.87	2.45
15	1.98	1.93	2.28
16	2.03	2.00	1.62
17	2.09	2.06	1.48
18	2.15	2.11	1.91
19	1.12	1.09	2.33
20	1.16	1.11	3.98
21	1.18	1.12	5.33
22	1.19	1.13	5.28
23	1.21	1.14	5.86
24	1.21	1.16	4.05
25	1.24	1.16	6.30
26	1.25	1.19	4.42
27	1.27	1.20	5.21
28	1.28	1.22	4.76
29	1.27	1.22	4.24

Model No	Factor of Safety		Difference (%)
	SLOPE/W	Geo 5	
30	1.29	1.24	4.02
31	1.26	1.25	0.95
32	1.33	1.27	4.44
33	1.36	1.28	5.67
34	1.37	1.29	5.77
35	1.34	1.31	2.46
36	1.08	1.02	5.12
37	1.03	0.97	5.55
38	0.98	0.93	5.49
39	0.94	0.89	5.22
40	0.87	0.82	5.96
41	0.79	0.77	2.78
42	0.73	0.73	0.00
43	0.69	0.68	1.59
44	0.66	0.65	1.96
45	0.63	0.61	2.87
46	1.12	1.08	3.74
47	1.12	1.08	3.74
48	1.12	1.08	3.74
49	1.12	1.08	3.74
50	1.12	1.08	3.74
51	1.12	1.08	3.74
52	1.12	1.08	3.74
53	1.12	1.08	3.74
54	1.12	1.08	3.74
55	1.08	1.04	4.06
56	0.99	0.97	1.52
57	0.97	0.92	5.45
58	0.91	0.88	3.61
59	0.89	0.85	4.60
60	0.86	0.83	3.04
61	0.85	0.81	5.15
62	0.84	0.80	4.31
63	0.83	0.79	5.16
64	1.20	1.16	3.09
65	1.37	1.30	4.83
66	1.52	1.45	4.67
67	1.68	1.60	4.59
68	1.83	1.76	3.98
69	1.96	1.90	3.21
70	2.10	2.05	2.19
71	2.31	2.20	4.89
72	2.38	2.28	4.16

In Tables 14-19, it can be seen that GEO5 is a more conservative analysis program. In average, GEO5 gives 5% smaller factor of safety value which will make this application more conservative and thus more safe for designing and analyzing more important slopes. In contrast, giving out a greater factor of safety by SLOPE/W makes it more useful for analyzing and designing slopes with lower degree of importance.

To find the reason of this difference, the failure slopes of the models have been studied by considering their length of failure arc. The lengths and their differences in percent have been calculated and given in Table 21. This differences have been calculated using following formula.

$$\text{Difference} = \frac{L_{SLOPE/W} - L_{Geo-5}}{L_{Geo-5}} * 100 \qquad \text{Equation 30}$$

Table 21. Differences in Length of Failure Surfaces between SLOPE/W and Geo 5

Model No.	Length of Failure Arc (m)		Difference (%)
	SLOPE/W	Geo 5	
1	6.694	5.902	11.84
2	7.193	5.938	17.46
3	7.397	5.999	18.89
4	7.397	6.103	17.49
5	7.415	6.039	18.55
6	7.619	6.169	19.04
7	7.619	6.177	18.93
8	6.621	6.174	6.75
9	7.340	6.187	15.71
10	7.844	6.271	20.05

Model No.	Length of Failure Arc (m)		Difference (%)
	SLOPE/W	Geo 5	
11	6.605	6.314	4.41
12	6.376	6.375	0.01
13	7.805	6.343	18.73
14	8.071	6.329	21.59
15	8.071	6.441	20.20
16	8.071	6.563	18.69
17	8.071	6.447	20.12
18	8.050	6.511	19.11
19	6.010	5.784	3.75
20	6.129	5.768	5.89
21	6.959	5.714	17.90
22	6.759	5.711	15.50
23	6.745	5.668	15.97
24	5.944	5.594	5.89
25	6.547	5.530	15.54
26	5.283	5.572	-5.47
27	6.390	5.557	13.05
28	6.454	5.494	14.87
29	5.059	5.426	-7.26
30	5.312	5.312	-0.01
31	5.466	5.303	2.98
32	5.600	5.360	4.28
33	6.036	5.294	12.30
34	5.997	5.239	12.64
35	4.901	5.274	-7.62
36	6.975	5.807	16.75
37	6.975	5.780	17.12
38	6.959	5.740	17.52
39	6.759	5.714	15.46
40	6.745	5.686	15.70
41	6.080	5.615	7.64
42	5.438	5.549	-2.05
43	5.247	5.504	-4.89
44	5.065	5.492	-8.43
45	5.693	5.287	7.14
46	6.694	5.863	12.41
47	6.694	5.863	12.41
48	6.694	5.863	12.41
49	6.694	5.863	12.41
50	6.694	5.863	12.41
51	6.694	5.863	12.41
52	6.694	5.863	12.41
53	6.694	5.863	12.41

Model No.	Length of Failure Arc (m)		Difference (%)
	SLOPE/W	Geo 5	
54	6.694	5.863	12.41
55	5.928	5.819	1.85
56	5.622	5.611	0.21
57	6.338	5.547	12.48
58	5.377	5.368	0.17
59	5.555	5.173	6.89
60	5.214	5.078	2.60
61	5.429	4.856	10.55
62	5.263	4.845	7.94
63	5.233	4.791	8.45
64	6.694	5.576	16.71
65	7.176	5.813	18.99
66	7.176	5.961	16.93
67	7.176	5.971	16.79
68	5.680	5.946	-4.68
69	5.586	6.031	-7.96
70	5.794	5.967	-3.00
71	7.176	5.974	16.76
72	6.975	5.917	15.16

From Table 21, it can be observed that in average, there is a 9.83% difference between the lengths of failure arcs in the two software programs. This difference is due to the different failure surface search methods that have been used in each program. Although the used methods are expected to give the same (real) failure surfaces, because of reducing the analysis time, the software developers use different accuracy levels, which lead into different failure surfaces and hence different FSs. However, as it can be noted from the values given in Table 21, the difference between SLOPE/W and GEO5 is acceptable from an engineering point of view.

4.7 Re-Analyzing the Previous Models by FLAC/Slope

In order to check the results from SLOPE/W and GEO5, 10% of the models have been randomly selected using “Randomness and Integrity Services Limited”

company's website (www.Random.Org), and these models were re-analyzed using the FLAC/Slope software. Considering that FLAC/Slope is not a completely LE method software, the result may demonstrate a difference between three software.

Table 22. Re-Analyze Models - FLAC/Slope

Model No	Factor of Safety			Difference of FLAC and	
	SLOPE/W	GEO5	FLAC/Slope	SLOPE/W (%)	GEO5 (%)
18	2.15	2.11	1.99	7.87	5.82
26	1.25	1.19	1.33	-6.67	-10.79
42	0.73	0.73	0.82	-10.76	-10.76
46	1.12	1.08	1.12	-0.09	-3.83
56	0.99	0.97	1.07	-8.12	-9.51
69	1.96	1.90	1.98	-0.81	-3.99
72	2.38	2.28	2.38	-0.21	-4.36

As it can be seen from Table 22, in average, there is approximately 4% difference between FLAC/Slope and the other two software programs, which is acceptable.

Moreover it is noticeable that, in 85% of the models, FSs obtained from FLAC/Slope is greater than the other two programs.

4.8 Locating Failure Surface

Geometry dictates that for locating the failure surface, at least two parameters related to failure surface need to be known. For this reason, length of failure arc, and slip surface entry point will be used. In the following sections correlation between soil strength parameters and length of failure arc as well as slip surface entry distance

will be studied to find a formula to make them known by knowing soil strength parameters.

As it has been discussed in the previous sections, in order to relate the slip surface to the soil strength parameters and slope geometry, a dimensionless variable called λ has been hired.

Up to this point, relation of Lambda to the slip surface has been explained as a qualitative value for how deep or shallow is the failure surface according to(Lin & Cao, 2011).

4.8.1 Length of Failure Arc, L

To find the relation between Lambda and length of failure arc, Figure 44 will be drawn based on the outcomes obtained from the SLOPE/W software.

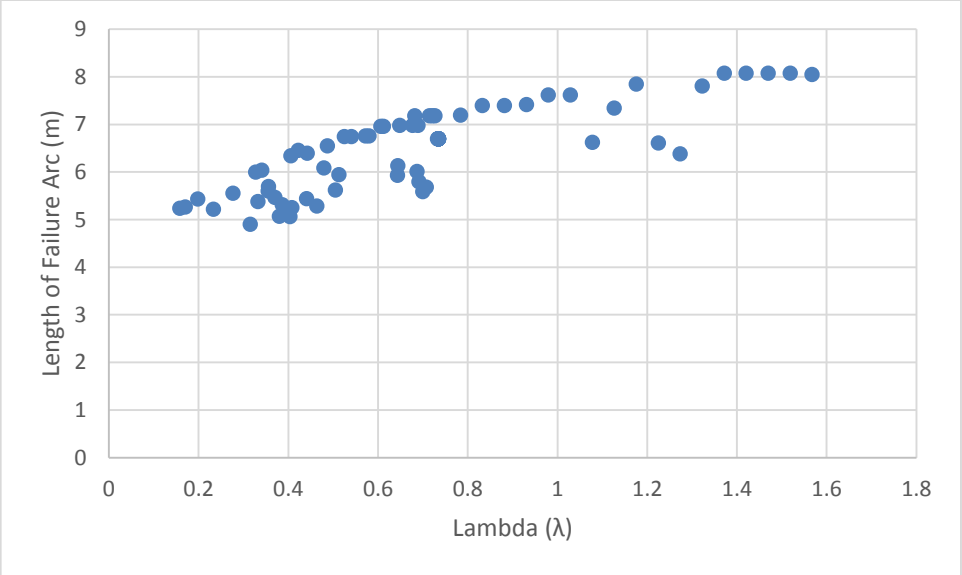

Figure 44. Length of Failure Arc vs. Lambda (λ) by SLOPE/W

Figure 45 gives the relationship between length of failure arc and lambda by using the data from GEO5 software.

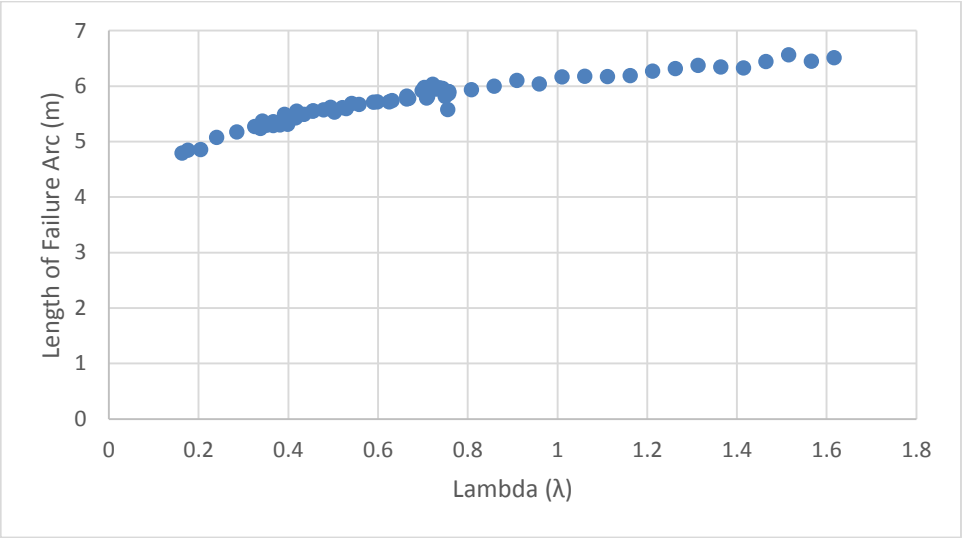

Figure 45. Length of Failure Arc vs. Lambda (λ) by GEO5

As it can be seen from these figures, both programs, represent a logarithmic trend line for the length if failure arc versus lambda. This trend is more obvious in Figure 45. The difference in lengths of arcs between two figures is due to the difference between the algorithms in which these programs uses to find the failure surface (as it has been explained in section 5.4).

The behavior in Figure 44, can be summarized as, the method which SLOPE/W uses to find the minimum safety factor is to draw circles with various radiuses (according to number of radius increments in Figure 15), crossing from two defined ranges (Entry and Exit points defined in Figure 15 and shown in red dots in Figure 17) which would result nearly 30,000 circles. Each circle would be analyzed and results into a factor of safety and accordingly the minimum found is the critical slip surface between these 30,000 candidates.

In other words, in this software (SLOPE/W), critical failure surface will be selected between a number of potential failure surfaces. This means that, no optimization technique has been used in this software, and hence, two critical failure surfaces relevant to two similar slopes (with similar soil strength parameters but different entry and exit range for the slip surface and/or radius increments) may be not be similar to each other.

On the other hand, in GEO5, an optimization technique is used, hence, slopes are more close to the real failure surfaces, although since finding the real failure surface is too much time consuming, application will stop the optimization at a desired accuracy level. This usage of the optimization technique, will give a more in trend data in L-λ figure (Figure 45).

Based on what that has been discussed in this section, the data which seem to be outliers actually can be considered as a reliable data (with an acceptable engineering tolerance) but in order to find a better trend line, these outliers will be omitted from the results and Figure 44 and Figure 45 will be re-drawn without considering these outliers.

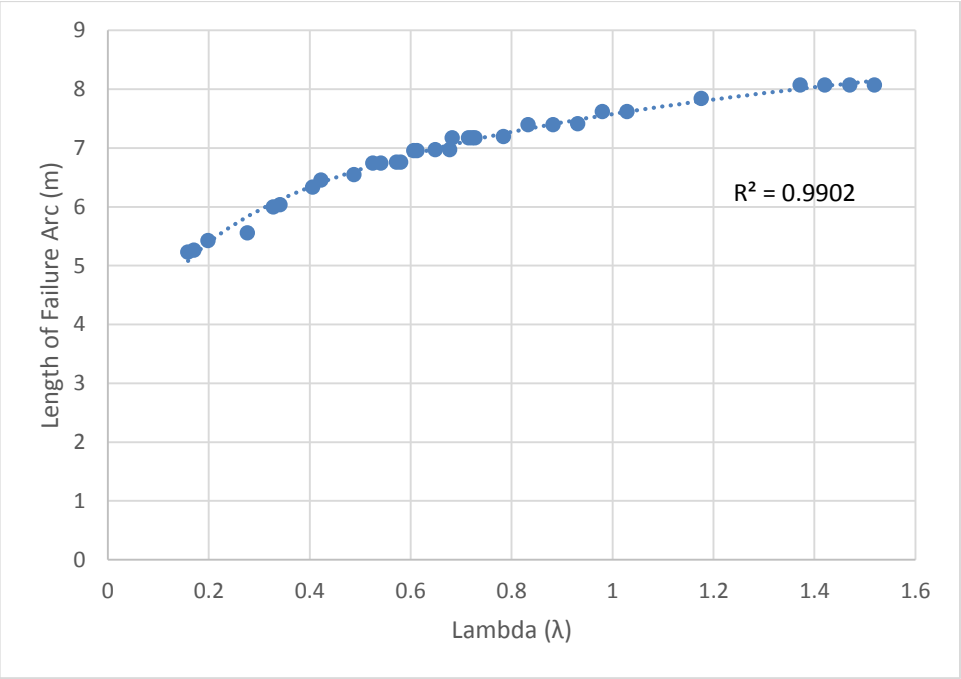

Figure 46. Length of Failure Arc vs. Lambda (λ) by SLOPE/W - No Outlier

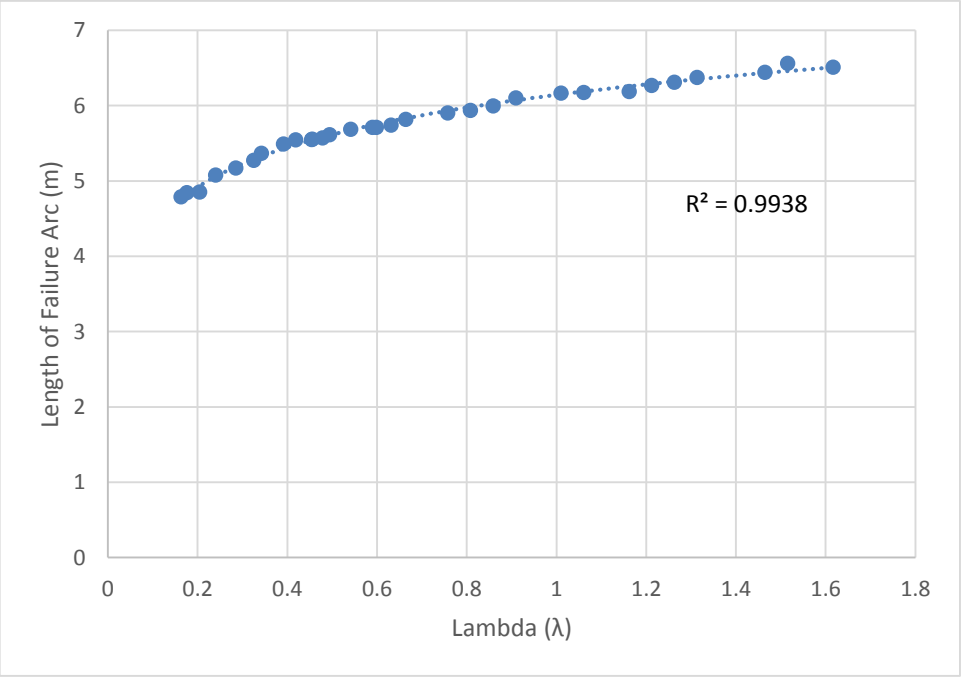

Figure 47. Length of Failure Arc vs. Lambda (λ) by GEO5 - No Outlier

Considering the above figures (Figure 46 and Figure 47), it can be accepted that there is a clear logarithmic relation between length of failure arc and the lambda parameter, and keeping in mind that lambda itself is a dimensionless parameter related to soil slope properties, it is safe to say that length of failure arc is predictable based on the slope properties using the following equation derived from a non-linear regression using SPSS software.

$$L = 0.76 \ln\left(\frac{c}{(\gamma\, h\, \mathrm{Tan}(\varphi))}\right) + 6.14 \qquad \text{Equation 31}$$

4.8.2 Slip Surface Entry Point Distance, l_e

As it has been discussed earlier, to locate the failure surface, two parameters: one of them is the length of the failure arc, and the other one is the entry point of the slip surface will be proposed in this study. For this purpose, the distance from the edge of the slope will be introduced as "1_e" as can be seen in Figure 48.

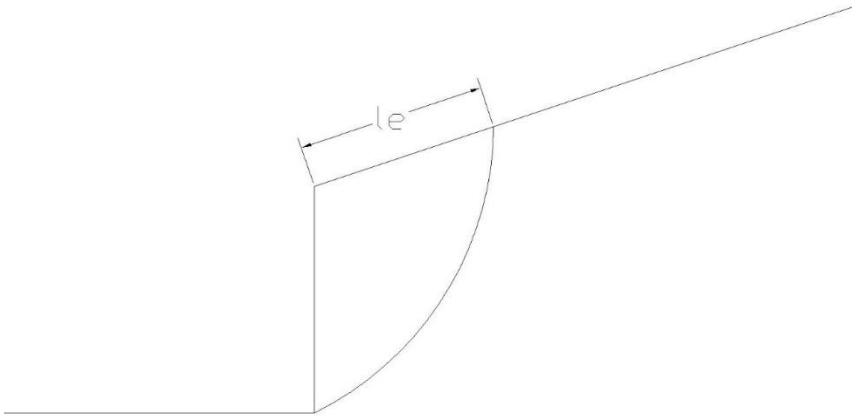

Figure 48. Slip Surface Entry Point Distance, l_e

As it can be seen in the Figure 49, there is a logarithmic relation between lambda and l_e. This figure has been drawn using 72 models, analyzed by GEO5 software.

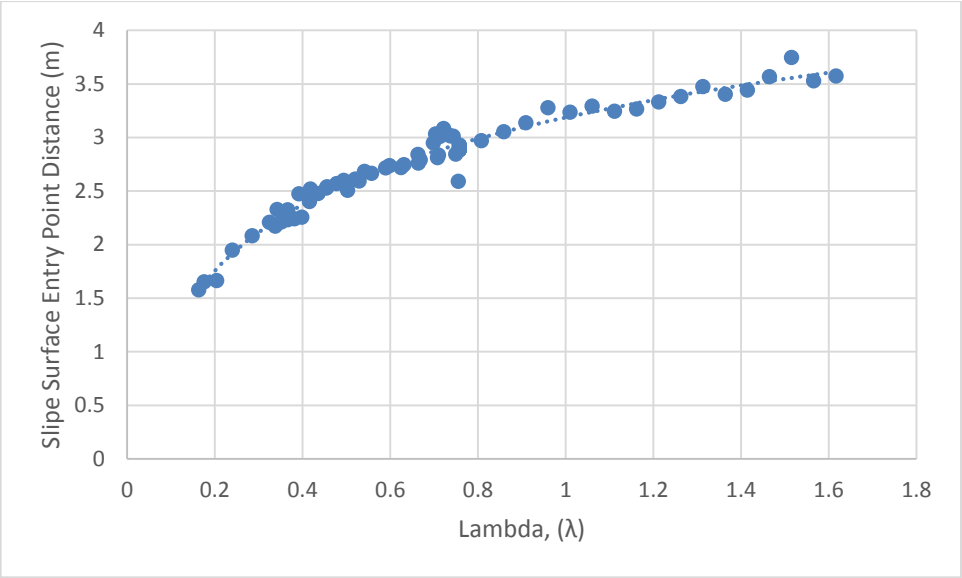

Figure 49. Lambda versus Slip Surface Entry Point Distance

With exactly the same reason, as discussed in section (4.8.1), regarding the reason for outliers in the length of failure arc figures (Figure 44 and Figure 45), Figure 50 can be redrawn by omitting the outliers in Figure 49.

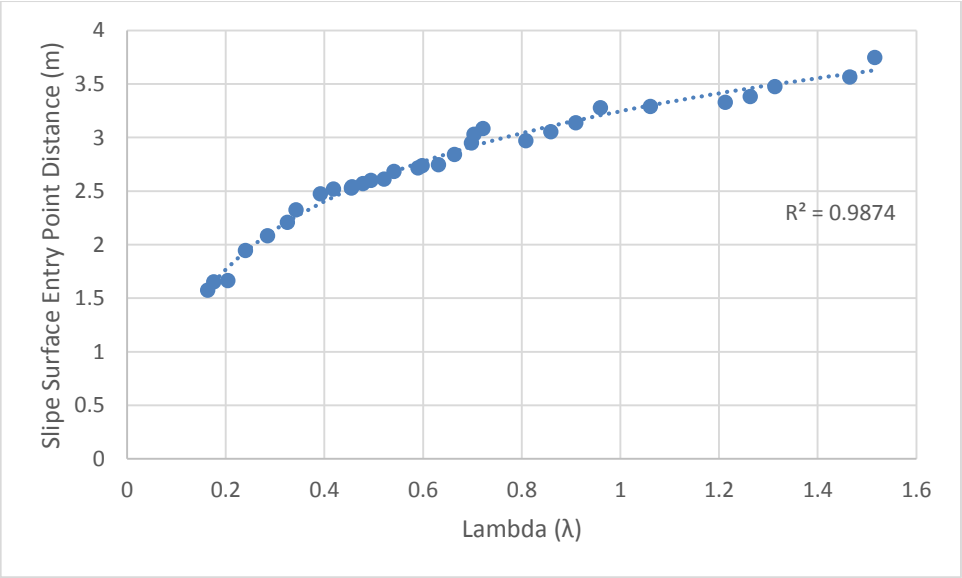

Figure 50. Lambda vs. Slip Surface Entry Point Distance – (No Outliers)

Considering Figure 50, it can be accepted that there is a clear logarithmic relation between slip surface entry point distance, l_e, and the lambda parameter, and keeping that in mind lambda itself is a dimensionless parameter related to soil slope properties, it is safe to say that slip surface entry point is predictable based on the slope properties using the following equation derived from a non-linear regression using SPSS software.

$$l_e = 0.91\, ln\left(\frac{c}{(\gamma\, h\, \mathrm{Tan}(\varphi))}\right) + 3.24 \qquad \text{Equation 32}$$

4.8.3 Locating Slip Surface

To locate the slip surface, the following geometrical study has been carried out. In Figure 51, K is the slip surface entry point and D is the exit point. Regarding the previous studies, D almost always is located on the lowest point of slope. Hence, "a" can be assumed to be equal to $h/\cos\beta$, in which "h" is the height of slope.

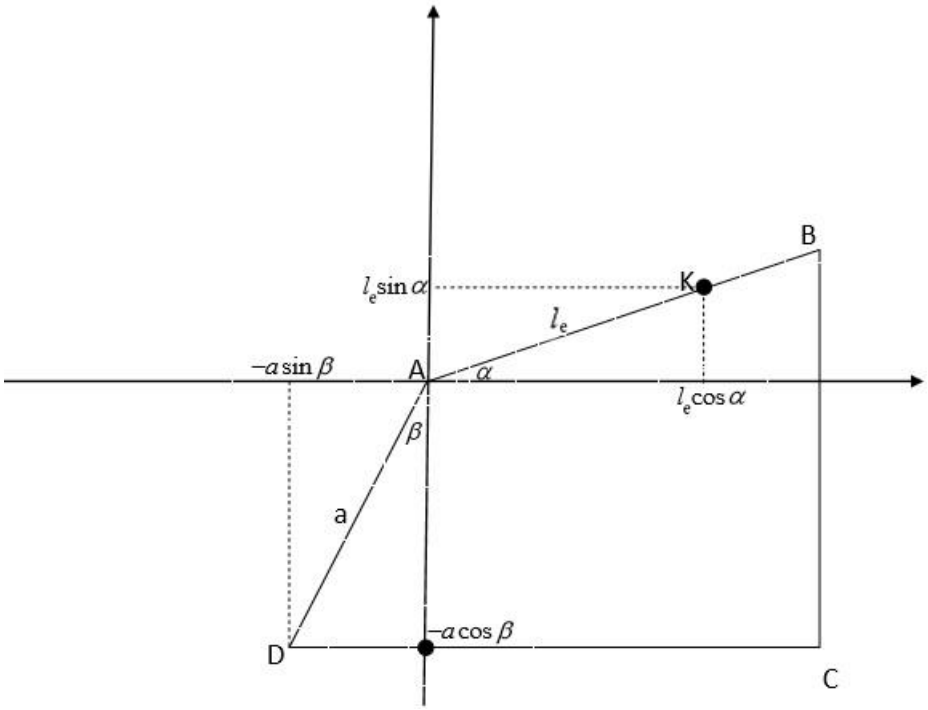

Figure 51. Slope Geometry

To solve this problem, we assume the following equation for the failure circle formula.

$$(x - x_0)^2 + (y - y_0)^2 = r^2 \qquad \text{Equation 33}$$

In Equation 33 x_0, y_0 and r are unknown variables so in order to find them, three equations are needed. Since entry and exit points shall satisfy the Equation 33, two of the equations will be created by inserting their coordinates in the Equation 33.

To create the third equation, length of the failure arc will be used as a known parameters (using Equation 31) and it will be inserted into the following formula of curve length integral.

Length of curve is equal to:

$$p = \int_{x_d}^{x_k} \sqrt{(1 + (y')^2}\, dx$$

in which p is the length of failure arc, L, and:

$$y' = \frac{x - x_0}{\sqrt{r^2 - (x - x_0)^2}}$$

Hence:

$$L = \int_{x_d}^{x_k} \frac{r}{\sqrt{r^2 - (x - x_0)^2}} dx$$

$$L = r\ (\sin^{-1} \frac{l_e \cos\alpha - x_0}{r} - \sin^{-1} \frac{-a\ \sin\beta - y_0}{r})$$

Hence, the three equations needed to calculate the coordinates of failure circle will be as follow:

$$\begin{cases} (l_e \cos\alpha - x_0)^2 + (l_e \sin\alpha - y_0)^2 = r^2 \\ (-a\cos\beta - x_0)^2 + (-a\sin\beta - y_0)^2 = r^2 \\ r\ \left(\sin^{-1} \frac{l_e \cos\alpha - x_0}{r} - \sin^{-1} \frac{-a\ \sin\beta - y_0}{r}\right) = L \end{cases}$$ Equation 34

By inserting known parameters (a, l_e, α, β, and L) the above equation system is solvable by numerical methods. The answer of this system will be x_0, y_0, and r which are the coordinates of failure circle center and its radius.

4.9 Relation between Factor of Safety and Length of Failure Arc

Analyzing output data in each section of the results may bring this idea to the mind that there might be a relation between factor of safety and length of failure arc. To study this idea, using results from GEO5 software, Figure 52 has been drawn and the relation between factor of safety and length of failure arc has been shown.

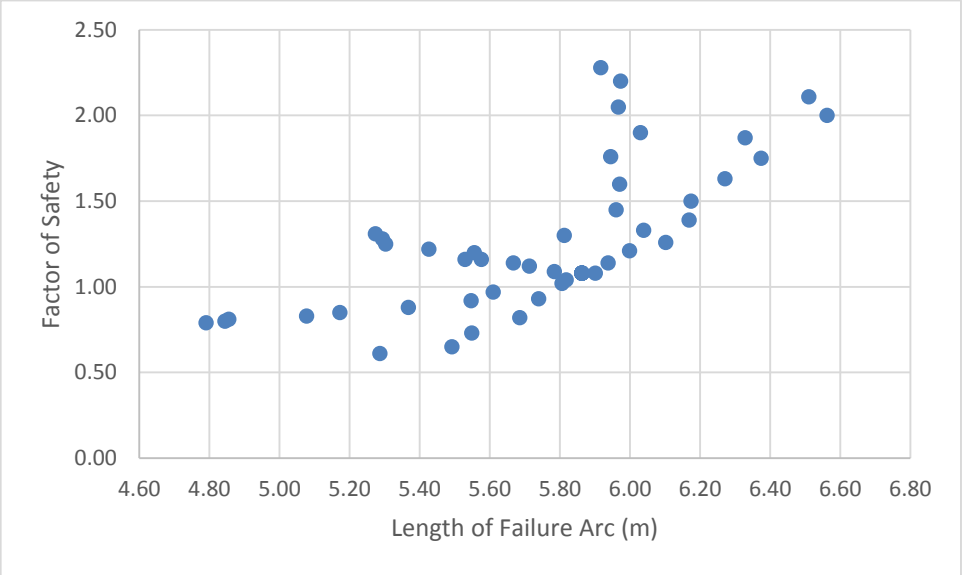

Figure 52. FS. vs. Length of Failure Arc

As it can be seen from Figure 52, there is no relation between factor of safety and the length of failure arc.

Chapter 5

CONCLUSIONS AND RECOMMENDATIONS FOR FURTHER STUDIES

5.1 Conclusions

Based on the slope stability analyses performed by using different software programs: SLOPE/W, GEO5 and FLAC/Slope, the following conclusions have been drawn:

1. Friction angle (φ) and cohesion (c), as resistance forces, are directly related to factor of safety while unit weight (γ), as driving force, is inversely related to factor of safety.
2. Increasing the value of cohesion (c) leads to an increase in the value of the length of failure arc (L).
3. Increasing the value of friction angle (φ) leads to a reduction in the value of the length of failure arc (L).
4. The greater unit weight of soil (γ) gets, the greater is the value of the length of failure arc (L).
5. Increasing the Alpha angle until a specific angle does not have any significant effect on the factor of safety. On the other hand, increasing the Beta angle directly affects the Factor of safety.

6. Increasing the Alpha angle, leads to an increase in the length of failure arc. However, changing the Beta angle does not significantly affect the length of failure arc.
7. GEO5 is more conservative slope stability analysis software, compared to SLOPE/W it gives 5% smaller factor of safety.
8. FLAC/Slope usually gives out greater value for factor of safety compared to SLOPE/W and GEO5.
9. Constant value of lambda (λ) results in constant factor of safety.
10. Constant value of lambda (λ) results in constant slip surface.
11. Greater value of lambda (λ) means a deeper slip surface and a greater value for length of failure arc (L). Oppositely, smaller value of lambda leads to more shallow slip surface and smaller value for the length of the failure arc.
12. There is no relation between factor of safety and length of failure arc (L).
13. The length of failure arc (L) is logarithmically related to lambda (λ) using following formula:

$$\mathrm{L} = 0.76 \ln\left(\frac{\mathrm{c}}{(\gamma\, \mathrm{h}\, \mathrm{Tan}(\varphi))}\right) + 6.14$$

14. The slip surface entry point distance from the slope edge (l_e) is also logarithmically related to lambda (λ). This correlation can be formulated as follow.

$$l_e = 0.91\, ln\left(\frac{\mathrm{c}}{(\gamma\, \mathrm{h}\, \mathrm{Tan}(\varphi))}\right) + 3.24$$

15. The failure surface can be found by solving the following equation system:

$$\begin{cases} (l_e \cos\alpha - x_0)^2 + (l_e \sin\alpha - y_0)^2 = r^2 \\ (-a\cos\beta - x_0)^2 + (-a\sin\beta - y_0)^2 = r^2 \\ r\left(\sin^{-1}\dfrac{l_e\cos\alpha - x_0}{r} - \sin^{-1}\dfrac{-a\ \sin\beta - y_0}{r}\right) = L \end{cases}$$

where x_0, y_0, are the coordinates of the failure circle center and r is the radius of the circle.

5.2 Limitations of This Study

In this study, due to time limitation, only a limited range of soil strength parameters have been studied. Moreover, because of the limitation of the available software programs, only the factors affecting the length of failure arcs have been studied.

5.3 Further Studies

Related to this thesis study, the following analysis can be performed for further studies:

1. Modeling and analyzing greater range in the soil strength parameters.
2. Including the water content level and furthermore considering the unsaturated soils and pore-air and water pressure effect.
3. Including more variables regarding the slope geometry (e.g. slope height)
4. Conducting a case study to check the validity of the obtained formula for locating the critical failure surface.

REFERENCES

Abramson, L. W. (2002). Slope stability and stabilization methods: John Wiley & Sons Inc.

Albataineh, N. (2006). Slope stability analysis using 2D and 3D methods. The University of Akron.

Alkema, D., & Hack, H. (2011). Stability assessment of man-made slopes, A case study in Yen Bai. (Master of Science), University of Twente.

Anagnosti, P. (1969). Three-dimensional stability of fill dams.

Anderson, M., & Richards, K. (1987). Modelling slope stability: the complimentary nature of geotechnical and geomorphological approaches. Slope Stability: Geotechnical Engineering and Geomorphology. John Wiley and Sons., 1-9.

Aryal, K. (2008). Differences between LE and FE methods used in slope stability evaluations. Paper presented at the The 12th International Conference of International Association for Computer Methods and Advances in Geomechanics (IACMAG).

Azadmanesh, M., & Arafati, N. (2012). A Comparison on Slope Stability Analysis of Aydoghmoosh Earth Dam by Limit Equilibrium, Finite Element and Finite Difference Methods. IJCEBM, 115-124.

Azzouz, A., Baligh, M., & Ladd, C. (1981). Three-dimensional stability analyses of four embankment failures. Paper presented at the Proceedings of the 10th International Conference on Soil Mechanics and Foundation Engineering, Volume 3, Stockholm.

Azzouz, A. S., & Baligh, M. M. (1983). Loaded areas on cohesive slopes. Journal of Geotechnical Engineering, 109(5), 724-729.

Baker, R. (1980). Determination of the critical slip surface in slope stability computations. International journal for numerical and analytical methods in geomechanics, 4(4), 333-359.

Baker, R., & Leshchinsky, D. (1987). Stability analysis of conical heaps. Soils and Foundations, 27(4), 99-110.

Baligh, M. M., & Azzouz, A. S. (1975). End effects on stability of cohesive slopes. Journal of the Geotechnical Engineering Division, 101(11), 1105-1117.

Baligh, M. M., Azzouz, A. S., & Ladd, C. C. (1977). Line loads on cohesive slopes.

Bojorque, J., De Roeck, G., & Maertens, J. (2008). Comments on 'Two-dimensional slope stability analysis by limit equilibrium and strength reduction methods' by Y.M. Cheng, T. Lansivaara and W.B. Wei [Computers and Geotechnics 34 (2007) 137–150]. Computers and Geotechnics, 35(2), 305-308.

Bolton, H., Heymann, G., & Groenwold, A. (2003). Global search for critical failure surface in slope stability analysis. Engineering Optimization, 35(1), 51-65.

Boutrup, E., & Lovell, C. (1980). Searching techniques in slope stability analysis. Engineering Geology, 16(1), 51-61.

Bromhead, E. (1992). The stability of slopes: Taylor & Francis.

Carter, R. (1971). Computer oriented slope stability analysis by method of slices. MSCE Thesis, Purdue University.

Cavoundis, S. (1987). On the ratio of factors of safety in slope stability analyses. Geotechnique, 37(2), 207-210.

Celestino, T., & Duncan, J. (1981). Simplified search for non-circular slip surface. Paper presented at the Proceedings of the 10th International Conference on Soil Mechanics and Foundation Engineering, Stockholm, Sweden.

Chen, R., & Chameau, J.-L. (1983). Three-dimensional limit equilibrium analysis of slopes. Geotechnique, 33(1), 31-40.

Cheng, Y. (2003). Location of critical failure surface and some further studies on slope stability analysis. Computers and Geotechnics, 30(3), 255-267.

Cheng, Y. (2008). Reply to "Comments on 'Two-dimensional slope stability analysis by limit equilibrium and strength reduction methods' by YM Cheng, T. Lansivaara

and WB Wei," by J. Bojorque, G. De Roeck and J. Maertens. Computers and Geotechnics, 35(2), 309.

Cheng, Y., Lansivaara, T., & Wei, W. (2007). Two-dimensional slope stability analysis by limit equilibrium and strength reduction methods. Computers and Geotechnics, 34(3), 137-150.

Cheng, Y., & Lau, C. (2008). Slope stability analysis and stabilization: new methods and insight: Psychology Press.

Cheng, Y., Li, L., Chi, S.-c., & Wei, W. (2007). Particle swarm optimization algorithm for the location of the critical non-circular failure surface in two-dimensional slope stability analysis. Computers and Geotechnics, 34(2), 92-103.

Cheng, Y., Li, L., Lansivaara, T., Chi, S., & Sun, Y. (2008). An improved harmony search minimization algorithm using different slip surface generation methods for slope stability analysis. Engineering Optimization, 40(2), 95-115.

Cheng, Y. M., Lansivaara, T., & Wei, W. B. (2007). Two-dimensional slope stability analysis by limit equilibrium and strength reduction methods. Computers and Geotechnics, 34(3), 137-150. doi: http://dx.doi.org/10.1016/j.compgeo.2006.10.011

Cho, S. E., & Lee, S. R. (2001). Instability of unsaturated soil slopes due to infiltration. Computers and Geotechnics, 28(3), 185-208.

Das, B. M. (2010). Principles of geotechnical engineering: Cl-Engineering.

Duncan, J. M. (1996). State of the art: limit equilibrium and finite-element analysis of slopes. Journal of Geotechnical Engineering, 122(7), 577-596.

Duncan, J. M., & Wright, S. G. (2005). Soil strength and slope stability: John Wiley & Sons, Incorporated.

Gens, A., Hutchinson, T., & Cavounidis, S. (1988). Three-dimensional analysis of slides in cohesive soils. Geotechnique, 38(1), 1-23.

Giger, M. W., & Krizek, R. J. (1976). Stability of vertical corner cut with concentrated surcharge load. Journal of the Geotechnical Engineering Division, 102(1), 31-40.

Goh, A. T. (1999). Genetic algorithm search for critical slip surface in multiple-wedge stability analysis. Canadian Geotechnical Journal, 36(2), 382-391.

Griffiths, D., & Lane, P. (1999). Slope stability analysis by finite elements. Geotechnique, 49(3), 387-403.

Griffiths, D., & Lu, N. (2005). Unsaturated slope stability analysis with steady infiltration or evaporation using elasto-plastic finite elements. International journal for numerical and analytical methods in geomechanics, 29(3), 249-267.

Hack, R., Alkema, D., Kruse, G. A., Leenders, N., & Luzi, L. (2007). Influence of earthquakes on the stability of slopes. Engineering geology, 91(1), 4-15.

Hovland, H. J. (1979). Three-dimensional slope stability analysis method. Journal of Geotechnical and Geoenvironmental Engineering, 105(ASCE 14549 Proceeding), 693-695.

Hungr, O. (1987). An extension of Bishop's simplified method of slope stability analysis to three dimensions. Geotechnique, 37(1), 113-117.

Jiang, J.-C., & Yamagami, T. (2006). Charts for estimating strength parameters from slips in homogeneous slopes. Computers and Geotechnics, 33(6), 294-304.

Jiang, J.-C., & Yamagami, T. (2008). A new back analysis of strength parameters from single slips. Computers and Geotechnics, 35(2), 286-291.

Jibson, R. W. (2011). Methods for assessing the stability of slopes during earthquakes—A retrospective. Engineering Geology, 122(1), 43-50.

Khabbaz, H. F., Behzad;Nucifora, C. (2012). Finite Element Methods against Limit Equilibrium Approaches for Slope Stability Analysis. Geomechanical Society and New Zealand Geotechnical Society, 5.

Leshchinsky, D., & Baker, R. (1986). Three-dimensional slope stability: end effects. Soils and Foundations, 26(4), 98-110.

Leshchinsky, D., Baker, R., & Silver, M. (1985). Three dimensional analysis of slope stability. International Journal for Numerical and Analytical Methods in Geomechanics, 9(3), 199-223.

Leshchinsky, D., & Huang, C.-C. (1992). Generalized three-dimensional slope-stability analysis. Journal of Geotechnical Engineering, 118(11), 1748-1764.

Li, K. S., & White, W. (1987). Rapid evaluation of the critical slip surface in slope stability problems. International Journal for Numerical and Analytical Methods in Geomechanics, 11(5), 449-473.

Lin, H., & Cao, P. (2011). Potential slip surfaces of slope with strength parameters. Advanced Materials Research, 243, 3315-3318.

Lin, H., & Cao, P. (2012). Limit Equilibrium Analysis for the Relationships Among Slope c, phi and Slip Surface. Electronic Journal of Geotechnical Engineering, 17, 185-195.

Malkawi, A. I. H., Hassan, W. F., & Sarma, S. K. (2001). Global search method for locating general slip surface using Monte Carlo techniques. Journal of Geotechnical and Geoenvironmental Engineering, 127(8), 688-698.

Matsui, T., & San, K. (1992). Finite element slope stability analysis by shear strength reduction technique. Soils and Foundations, 32(1), 59-70.

McCombie, P., & Wilkinson, P. (2002). The use of the simple genetic algorithm in finding the critical factor of safety in slope stability analysis. Computers and Geotechnics, 29(8), 699-714.

Michalowski, R. (1989). Three-dimensional analysis of locally loaded slopes. Geotechnique, 39(1), 27-38.

Namdar, A. (2011). Geometry in Slope Modeling and Design. e -Journal of Science & Technology (e-JST)(22), 9-21.

Nguyen, V. U. (1985). Determination of critical slope failure surfaces. Journal of Geotechnical Engineering, 111(2), 238-250.

Revilla, J., & Castillo, E. (1977). The calculus of variations applied to stability of slopes. Geotechnique, 27(1), 1-11.

Seed, R. B., Mitchell, J. K., & Seed, H. B. (1990). Kettleman hills waste landfill slope failure. II: stability analyses. Journal of Geotechnical Engineering, 116(4), 669-690.

Sengupta, A., & Upadhyay, A. (2009). Locating the critical failure surface in a slope stability analysis by genetic algorithm. Applied Soft Computing, 9(1), 387-392.

Siegel, R. A. (1975). Computer analysis of general slope stability problems: Indiana Department of Transportation and Purdue

University.

Spencer, E. (1967). A method of analysis of the stability of embankments assuming parallel inter-slice forces. Geotechnique, 17(1), 11-26.

Swan, C. C., & Seo, Y. K. (1999). Limit state analysis of earthen slopes using dual continuum/FEM approaches. International journal for numerical and analytical methods in geomechanics, 23(12), 1359-1371.

Ugai, K. (1985). Three-dimensional stability analysis of vertical cohesive slopes. Soils and Foundations, 25(3), 41-48.

Ugai, K. (1988). Three-dimensional slope stability analysis by slice methods. Paper presented at the Proceedings of the Sixth International Conference on Numerical Methods in Geomechanics (Vol. 2, pp. 1369-1374).

Whitman, R. V., & Bailey, W. A. (1967). Use of computers for slope stability analysis. Journal of Soil Mechanics & Foundations Div.

Wright, S. G. (1969). A study of slope stability and the undrained shear strength of clay shales. University of California, Berkeley.

Wright, S. G., Kulhawy, F. H., & Duncan, J. M. (1973). Accuracy of equilibrium slope stability analysis. Journal of the Soil Mechanics and Foundations Division, 99(10), 783-791.

Xing, Z. (1988). Three-dimensional stability analysis of concave slopes in plan view. Journal of Geotechnical Engineering, 114(6), 658-671.

Zolfaghari, A. R., Heath, A. C., & McCombie, P. F. (2005). Simple genetic algorithm search for critical non-circular failure surface in slope stability analysis. Computers and Geotechnics, 32(3), 139-152.